

NASA Technical Paper 1194

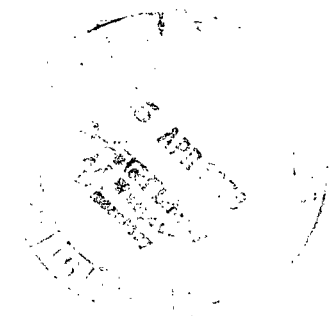
TECH LIBRARY KAFB, NM  
0134551

LOAN COPY: RETURN  
AFWL TECHNICAL LIBRARY  
KIRTLAND AFB, N. M.

# Performance of a Short Annular Dump Diffuser Using Suction-Stabilized Vortices at Inlet Mach Numbers to 0.41

John M. Smith and Albert J. Juhasz

APRIL 1978





NASA Technical Paper 1194

Performance of a Short  
Annular Dump Diffuser Using  
Suction-Stabilized Vortices  
at Inlet Mach Numbers to 0.41

John M. Smith and Albert J. Juhasz  
*Lewis Research Center*  
*Cleveland, Ohio*

**NASA**

National Aeronautics  
and Space Administration

**Scientific and Technical  
Information Office**

1978

PERFORMANCE OF A SHORT ANNULAR DUMP DIFFUSER USING  
SUCTION-STABILIZED VORTICES AT INLET  
MACH NUMBERS TO 0.41

by John M. Smith and Albert J. Juhasz  
Lewis Research Center

SUMMARY

A short, annular dump diffuser was designed to use suction to establish stabilized vortices on both walls for improved flow expansion in the region of an abrupt area change. The diffuser was tested at near ambient inlet pressure and temperature. Velocity profiles and diffuser pressure recovery performance data were obtained for nominal inlet Mach numbers of 0.18 to 0.41 with suction rates from 0 to 18 percent of the total inlet airflow. The prediffuser section had an included divergence angle of  $14^\circ$  and a length of 1.65 times the diffuser inlet height of 2.54 centimeters, resulting in a prediffuser area ratio of 1.4. The overall ratio of diffuser exit area to diffuser inlet area was 4.0. The overall ratio of diffuser length to inlet height was determined by the location of a variable-position vortex ring, or fence, and varied from 1.85 to 2.05 times the inlet height. Exit velocity profile and pressure measurements were taken downstream of the vortex fence at a distance equal to either two or six times the inlet height.

Test results show that the diffuser exit velocity profiles were typical of an annular jet without suction. However, they could be flattened and the peak velocity shifted toward tip (outer wall) or hub (inner wall) by varying the amounts of outer- and inner-wall suction. Symmetric exit velocity profiles were difficult to obtain and were inherently unstable. The profiles would slowly change to either a hub-weighted or tip-weighted profile.

Diffuser effectiveness, that is, diffuser static pressure recovery, was increased from about 47 percent without suction to approximately 87 percent at a total suction rate of about 14 percent, depending on the dimensions of the gap between the vortex fence and the end of the prediffuser. The diffuser total pressure losses were reduced from 1.1 and 5.6 percent at inlet Mach numbers of 0.18 and 0.41 without suction to 0.48 and 5.2 percent at total suction rates of 14.4 and 5.6 percent, respectively.

## INTRODUCTION

An investigation was conducted to determine the performance of a short, annular dump diffuser with improved flow expansion by using suction to provide stable vortices.

Ringleb (ref. 1) proposed the use of standing vortices to control flow expansion because of his observations of mountain ridge vortex flows, which cause snow cornice formation. In his design with contoured cusps in the wall of the diffuser to trap and hold a vortex, no replacement of energy lost to wall friction was available. In reference 2, Heskestad reports this diffuser was limited in performance due to difficulty in maintaining stable vortices. He tested a two-dimensional duct with a variable-step area change on its lower wall followed by a suction slot (ref. 2). The tests showed that a smooth expansion of the flow without separation downstream of the step area change could be obtained without cusps if sufficient suction was applied. These results were confirmed by Heskestad (ref. 3) in tests using suction on flow through a pipe with an abrupt area change. Suction slot design determined the amount of suction required. The optimum slot design from reference 3 was used to test an annular diffuser with an abrupt area change (ref. 4). Diffuser performance was improved, but the results indicated that stable vortices had not formed. In reference 5, a perforated plate placed downstream of the diffuser dump plane was found to improve the diffuser performance and to help form stable vortices. The results showed that stable vortices could be maintained if a solid wall was located downstream of the vortex. Similar results were recorded in reference 6 for an annular step-area-change diffuser; flat walls called fences were placed downstream of the vortices, which were formed and stabilized by suction. The fences formed a partially enclosed vortex chamber with the upstream walls of the diffuser. As reported in reference 7, detailed performance data were obtained from a modified version of the diffuser used in references 4 and 5.

Metal rings, or fences, of varying height were mounted to form a partially enclosed vortex chamber. These rings could be moved axially to vary the width of the slot. The present investigation was performed with the same diffuser as was used in a previous investigation (ref. 7), with the exception that the prediffuser included divergence angle was increased to  $14^{\circ}$ . As a result of this modification, the prediffuser area ratio was increased from 1.15 to 1.4. The diffuser inlet passage height was 2.54 centimeters. The overall diffuser area ratio was 4.0 and the prediffuser length was 1.65 times the diffuser inlet height. The diffuser inlet passage flow area was 304 square centimeters.

Radial profiles of velocity and diffuser effectiveness (static pressure recovery) and total pressure loss data were obtained for nominal Mach numbers of 0.18, 0.26, 0.30, 0.34, and 0.41 with suction rates from 0 to 18 percent of total airflow. The testing was conducted at ambient temperature and pressure.

## SYMBOLS

A	area
AR	diffuser area ratio
B	bleed flow fraction of total flow rate
$C_p$	specific heat at constant pressure
$g_c$	dimensional constant
H	diffuser inlet passage height
L	distance from vortex fence to exit pitot-static rakes
M	average Mach numbers at an axial station
m	mass flow rate
P	average pressure at an axial station
p	local pressure at a radial position
R	gas constant for air
S	suction rate, percent
T	temperature
V	average velocity at an axial station
v	local velocity at a radial station
x	axial distance from vortex fence to exit of prediffuser
y	radial distance of vortex fence to exit of prediffuser
$\gamma$	specific-heat ratio
$\epsilon$	diffuser efficiency
$\eta$	diffuser effectiveness

### Subscripts:

i	inner wall
m	maximum
o	outer wall
r	local value at given radial position
s	isentropic condition
t	total suction

- 0 total pressure and temperature
- 1 diffuser inlet station
- 2 diffuser exit station

## APPARATUS AND INSTRUMENTATION

### Flow System

The investigation was conducted in the test facility described in reference 4. A schematic of the test facility flow system is shown in figure 1. Ambient temperature air, at a pressure of approximately 1.0 megapascal absolute, is supplied to the facility by a remotely located compressor station. This air feeds the three branches of the flow system.

The center branch, called the main air line, provides the airflow through the test diffuser. The air flowing through this branch is metered by a square-edged orifice installed with flange taps according to ASME standards. The air is then throttled to near atmospheric pressure by a flow control valve before it enters a mixing chamber, from which it flows through the test diffuser. The air discharging from the diffuser is exhausted to the atmosphere through a noise-absorbing duct.

The two other branches of the flow system supply the two air ejectors, which produce the required vacuum for the inner- and outer-wall diffuser suction. The ejectors are designed for a supply air pressure of 0.68 megapascal absolute and are capable of producing absolute pressures as low as 0.0238 megapascal. The diffuser inner- and outer-wall suction is also metered by square-edged orifices. These orifices were installed with flange taps, according to ASME specifications, in the suction flow lines that connect the diffuser inner- and outer-wall suction chambers to their respective ejector vacuum sources.

### Diffuser Test Apparatus

The diffuser test apparatus used in this investigation was essentially that used in reference 4 except for the increased prediffuser included divergence angle and the increased prediffuser area ratio. An axial section of the apparatus is shown in figure 2. As in reference 4 the centerbody that formed the inner annular surface was cantilevered from eight equally spaced support struts located 30.5 centimeters upstream of the diffuser inlet passage. This construction minimized the possibility of strut flow separation having an undesirable effect on the circumferential profile of inlet velocity.

Diffuser walls. - The removable walls forming the prediffuser passage were positioned as shown in figure 2. The wall geometry and the suction slots formed by the prediffuser walls and the vortex fences are shown in figure 3. The diffuser inlet height was 2.54 centimeters. The vortex fence on each wall consisted of flat metal rings. The radial gap between the trailing edge of the prediffuser and the top of the vortex fence is referred to as the  $y$  dimension in figure 3. This dimension was varied from -0.02 to 0.15 times the diffuser inlet height  $H$ , based on results of similar diffuser tests in reference 7. Both vortex fences were positioned at axial distances from the trailing edge of the prediffuser  $x$  of 0.2, 0.3, and 0.4 times the diffuser inlet height, as indicated in figure 3. The annular prediffuser was designed with an included divergence angle of  $14^\circ$ , resulting in a prediffuser area ratio of 1.4 at a length-to-inlet-height ratio of 1.65.

The overall diffuser area ratio was 4.0. The overall diffuser length depended on the position of the exit instrumentation. The instrumentation was located downstream of the vortex fence at a distance of two or six times the inlet height ( $L/H = 2$  or  $6$ ). The vortex fence and the upstream walls of the diffuser formed the partially enclosed inner and outer suction chambers.

Diffuser instrumentation. - The basic diffuser instrumentation is shown in figures 2 and 3. Diffuser inlet total pressure was obtained from three five-point total pressure rakes located at the diffuser inlet station and spaced equally around the annular circumference. Inlet static pressure was measured by three wall taps also located at the diffuser inlet station.

Diffuser exit total and static pressures were obtained from three nine-point pitot static rakes that could be rotated in a circumferential direction and translated axially. For this investigation, these rakes were located downstream of the diffuser inlet plane at a distance equal to either two or six times the inlet passage height ( $L/H = 2$  or  $6$ ). All rake pressures were measured by three Scanivalves, each ducting pressures from a maximum of 48 ports to a flush-mounted,  $\pm 0.0069$ -megapascal strain-gage transducer. The valve dwell time at each port was 0.2 second, which is over three times the interval required to reach steady state. Continuous calibration of the Scanivalve system was provided by ducting known pressures to several ports. Visual display of pressure profiles was made available by connecting all inlet rakes and two exit rakes to common well manometers. The manometer fluid was dibutyl phthalate (specific gravity, 1.04). In addition, flow behavior in the diffuser exit passage could be monitored with tufts.

All other pressure data, such as orifice line pressures for the main air line and the subatmospheric suction flow lines, were obtained from individual strain-gage pressure transducers. The temperatures of the various flows were measured with copper-constantan thermocouples.

All data were remotely recorded on magnetic tape for subsequent processing with a

digital data reduction program. Any test parameter could also be displayed in the facility control room by means of a digital voltmeter.

## PROCEDURE

By using the digital data reduction program mentioned previously, the overall diffuser performance was evaluated in terms of the radial profile of exit velocity, the diffuser effectiveness, the total pressure loss, and the diffuser efficiency. The values of the last three quantities, or computations, were expressed in percentages. Intermediate computations included average static and total pressures, local and average Mach numbers, and local-to-average Mach number ratios, that is, the equivalent of the local to average velocity ratios. The average pressures and Mach numbers at the diffuser exit  $P_2$ ,  $P_{0,2}$ , and  $M_2$  were computed by trapezoidal integration using area-ratio-weighted pressures at the various radial positions. At the diffuser inlet, arithmetic averages were computed. Local Mach numbers for each pitot tube were computed from the compressible flow relation,

$$M_r = \sqrt{\frac{2}{\gamma - 1} \left( \frac{p_0}{p} \right)^{(\gamma-1)/\gamma} - 1} \quad (1)$$

where  $p_0$  and  $p$  are the measured local total and static pressures and  $\gamma$  is the specific-heat ratio, which was set equal to 1.4 for the near ambient conditions of this investigation.

Diffuser and bleed airflow rates were computed from the respective orifice pressures and temperatures. As a check on the arithmetically averaged inlet Mach number, a mean effective inlet Mach number was also computed by iteration from inlet airflow rate, total pressure and temperature, and area data as they relate in the expression

$$M_1 = \frac{m_1}{P_{0,1} A_1} \sqrt{\frac{RT_{0,1}}{\gamma g_c} \left( 1 + \frac{\gamma - 1}{2} M_1^2 \right)^{(\gamma+1)/2(\gamma-1)}} \quad (2)$$

The velocity ratios at each radial position, needed to generate velocity profiles, were obtained from the circumferential averages of the local-to-average Mach number ratios. A plotting routine was used to generate the velocity profiles by computer with output on microfilm. Diffuser effectiveness was computed from the relation



$$\eta = \frac{P_2 - P_1}{(P_{0,1} - P_1) \left(1 - \frac{1 - B^2}{AR}\right)} \times 100 \quad (3)$$

Equation (3) is an approximation expressing the ratio of actual to ideal conversion of inlet dynamic pressure to exit static pressure for the case of compressible flows through a diffuser with wall bleed for  $M \leq 0.5$  and  $AR \geq 2$ . For the conditions of the present study, using equation (3) introduced an approximation error of less than 0.6 percent. The derivation of equation (3) and its limitations are shown in reference 7.

The total pressure loss was defined as

$$\frac{\Delta P_0}{P_{0,1}} = \frac{P_{0,1} - P_{0,2}}{P_{0,1}} \times 100 \quad (4)$$

Diffuser efficiency was computed from the relation

$$\epsilon = \frac{\left(1 + \frac{\gamma - 1}{2} M_1^2\right) \left(\frac{P_{0,2}}{P_{0,1}}\right)^{(\gamma-1)/\gamma} - 1}{\frac{\gamma - 1}{2} M_1^2} \times 100 \quad (5)$$

Equation (5) was derived in reference 7 for the case where the diffuser exit velocity is negligible. This restriction can be removed from equation (5) (as shown in ref. 7) by a minor change in the definition and subsequent derivation of the diffuser efficiency parameter. Hence, equation (5), as used in this report, relates the total energy level available at the exit of the diffuser to the upstream total energy level, with the inlet static enthalpy being the reference.

## TEST CONDITIONS

The range of test conditions for this program is

Total pressure, MPa . . . . .	$9.95 \times 10^{-2}$ to $10.49 \times 10^{-2}$
Static pressure, MPa . . . . .	$9.15 \times 10^{-2}$ to $9.86 \times 10^{-2}$
Temperature, K . . . . .	275 to 293
Mach number . . . . .	0.18 to 0.41

Velocity, m/sec . . . . .	62 to 134
Reynolds number (based on inlet passage height) . . . . .	$2.0 \times 10^5$ to $4.8 \times 10^5$
Suction rate, percent of total flow . . . . .	0 to 18

The U.S. customary system of units was used for primary measurements and calculations. Conversion to SI units (Système International d'Unités) was done for reporting purposes only. In making the conversion, consideration was given to implied accuracy, which may have resulted in rounding off the values expressed in SI units.

## RESULTS AND DISCUSSION

The performance of a high-area-ratio dump diffuser that uses suction to establish stable vortices for flow control was tested over a range of Mach numbers to evaluate the following: radial profiles of velocity at inlet and exit planes, including circumferential effects; diffuser effectiveness, that is, static pressure recovery; diffuser efficiency; and diffuser total pressure loss. The data were obtained at nominal Mach numbers of 0.18, 0.26, 0.30, 0.34, and 0.41. There was no significant inlet Mach number effect on the performance parameters evaluated. The initial part of the test program was performed to find the vortex fence position and height that would give the highest diffuser effectiveness at the lowest pressure loss. Diffuser performance was then evaluated for this geometry. Because of facility limitations, the available suction rate decreased from about 18 percent at Mach 0.18 to about 5 percent at Mach 0.4. This limitation is reflected in the data plots and in the summary of performance data shown in tables I to IV.

### Diffuser Vortex Chamber Screening Tests

The effect of the vortex chamber geometry on diffuser performance was determined by varying the radial gap,  $y = (-0.02, 0.05, 0.10, \text{ and } 0.15)H$ , and the axial gap,  $x = (0.2, 0.3, \text{ and } 0.4)H$ , as measured from the exit of the prediffuser to the vortex fence. Results of these tests are listed in table I. As shown in figure 4, the radial gap  $y$  was varied over the range of values previously mentioned while the axial gap  $x$  was held at a constant value of  $0.3 H$ . This value for  $x$  was obtained from the results of testing the same diffuser with a smaller area ratio of 1.15 (ref. 7). From each of the curves in figure 4, values of diffuser effectiveness were selected for constant percentages of the diffuser total suction rate  $S_t$  of 4, 6, 8, 10, and 14 percent. These values of effectiveness were plotted against the corresponding values of radial gap  $y$  in figure 5. Although the diffuser effectiveness is slightly higher at  $y = -0.02 H$  than at

$y = 0.05 H$  for an  $S_t$  of 14 percent, the reverse is true for the other suction rates. Based on these diffuser effectiveness values, the best value for the radial gap  $y$  was chosen as  $0.05 H$ . The negative  $y$  value indicates that the edge of the fence is projecting into the main stream.

To verify that the best value of  $x$  was  $0.3 H$ , additional data were obtained at  $x$  of  $0.2 H$  and  $0.4 H$ , respectively, with  $y$  equal to  $0.05 H$ . Diffuser performances for these conditions are listed in table II. These results are shown in figure 6. From the data in figures 4(a) and 6(a) and (b), values of diffuser effectiveness were again selected for constant  $S_t$  of 4, 6, 8, 10, and 14 percent. The results are shown in figure 7. The values of diffuser effectiveness for  $x$  of  $0.3 H$  and  $0.4 H$  are approximately equal. The best value of  $x$  was arbitrarily chosen as  $0.3 H$  with  $y$  equal to  $0.05 H$ . These values of  $x$  and  $y$  were used in all subsequent testing.

### Radial Profiles of Inlet Velocity

The profiles shown in figure 8 were generated by plotting the ratio of local velocity at a radial probe position to the average velocity at the inlet station for several inlet Mach numbers. Figure 8 shows that inlet Mach number has no effect on the inlet velocity profiles. Profiles in three different circumferential planes as measured by the three equally spaced inlet plane rakes are shown on the right side of the figure. The circumferentially averaged profile is shown on the left side. Diffuser effectiveness for each of the rake positions is shown in the key to each part of figure 8.

There was little circumferential nonuniformity for the individual rake profiles with no suction for Mach numbers of 0.18 and 0.41 (figs. 8(a) and (b)). The profiles show a mild hub bias, which is characteristic of flow in annular passages, as discussed in reference 8. When the total suction rate was increased to approximately 14.5 percent, there was a change in the nonuniformity of the inlet profiles. This nonuniformity first appeared at total suction rates above 10 percent. In figure 8(c), the velocity profile at  $240^\circ$  shows some nonuniformity, although the effectiveness values are all high. But, in figure 8(d), for a slightly higher suction rate, the velocity profile at  $120^\circ$  shows a marked nonuniformity and the effectiveness value at this location is lower. This indicates that a separated region has been established downstream of rake 2, and it causes a decrease of the diffuser inlet flow in the rake 2 sector. Contrary to experience with other diffuser geometries (refs. 9 and 10), the vortex flow diffuser has a limiting suction rate beyond which performance deteriorates. This limiting suction rate was about 14 percent for the best conditions of this investigation. In addition, this is the first time that the use of suction has been observed to severely affect the prediffuser inlet velocity profile. This unusual result was not expected and cannot be satisfactorily explained.

## Radial Profiles of Exit Velocity

The radial profiles of exit velocity with no suction are shown in figure 9 for a nominal Mach number of 0.18 for exit rakes located at an  $L/H$  of 6. Circumferentially averaged inlet profiles are shown in each part. Figure 9(a) shows hub-weighted circumferentially averaged radial profiles. Figure 9(b) shows the three rake profiles circumferentially spaced at  $120^\circ$  intervals in the diffuser exit plane and the circumferential nonuniformity of the flow in the diffuser exhaust. By removing suction to either the inner- or outer-wall vortex chamber, either tip- or hub-weighted profiles could be obtained. Figure 10 shows this effect for a total suction rate of approximately 6.2 percent. Approximately 40 percent of the total suction was applied to the inner wall and 60 percent to the outer wall. For total suction rates to approximately 9 percent, with 40 percent of the total suction on the inner wall and 60 percent on the outer wall, either hub- or tip-weighted radial profiles were maintained, depending on the profile existing without suction. The hub-weighted profile of figure 10(b) resulted when the outer-wall suction used to obtain figure 10(a) was momentarily stopped and then reestablished before recording data. Similarly, the tip-weighted profiles of figure 11(b) resulted when the inner-wall suction used to obtain figure 11(a) was momentarily stopped and then reestablished before recording data. Either hub- or tip-weighted profiles could be generated by interrupting suction on the outer or inner wall, respectively.

Diffuser bleed schemes to control the combustor inlet velocity profile, as discussed in reference 11, may also use this ability to alter the radial profile of the combustor inlet velocity from hub- to tip-weighted by momentary, rather than steady, application of outer-wall suction. Alternatively, the process could be reversed by momentary application of inner-wall suction. In this manner, combustor airflow distribution could be controlled to suit the requirement of particular operating conditions without the penalty in engine cycle efficiency that would be incurred by a steady application of suction. At 13.7 percent total suction, the circumferential flow field is no longer biased toward either wall as a whole but is divided into a number of regions. Within each region the flow may be hub- or tip-weighted or may even periodically oscillate between the two extremes in a quasi-stable fashion. Evidence of such circumferentially segmented flow is shown in figure 12. Figure 12(a) shows the circumferentially averaged radial profile, which indicates the flow is attached to both walls. But in figure 12(b), which shows the radial profile at three circumferential locations, the  $120^\circ$  location indicates a hub-weighted profile attached only to the inner wall, while the  $240^\circ$  location indicates a tip-weighted profile attached only to the outer wall. At the  $0^\circ$  location, the flow is attached to both walls.

## Circumferential Variation of Exit Velocity Profiles

To determine circumferential variation in exit velocity profiles, a survey was made of the annular exhaust passage at  $10^\circ$  increments, using the nine-point exit pitot-static rakes. Figure 13(a) shows the circumferentially segmented flow obtained at a total suction rate of 10.2 percent. The flow field no longer has uniformly hub- or tip-weighted velocity profiles but is divided into sectors comprising outer-wall attachment (tip weighted); inner-wall attachment (hub weighted); and flow attached to both walls, which was inherently unstable. From  $0^\circ$  to  $120^\circ$  the flow is attached to both walls. From  $120^\circ$  to  $250^\circ$  the flow is hub weighted. From  $250^\circ$  to  $300^\circ$  the flow is again attached to both walls. From  $310^\circ$  to  $320^\circ$  the flow is tip weighted. From  $320^\circ$  to  $360^\circ$  the flow is again attached to both walls. Of the different flow patterns determined from these circumferential surveys, the hub-weighted profiles were most stable; the flows attached to both walls were unstable and underwent random oscillations from tip to hub attachment. Figure 13(b) shows more of the same circumferential variation for a total suction rate of 14.5 percent. The normal locations for the three nine-point pitot-static rakes were  $0^\circ$ ,  $120^\circ$ , and  $240^\circ$ . As shown in figure 13, circumferential flow conditions for suction rates greater than 10 percent could not be accurately measured with fixed rakes. Figure 14 shows the local to average velocity ratios for a probe position equal to 50 percent of the inlet height. In figure 14(a), for a total suction rate of 10.2 percent, there appears to be flow at all circumferential locations. In figure 14(b), for a total suction rate of 14.2 percent, there is a sector from about  $30^\circ$  to  $70^\circ$  where the flow is either low or nonexistent. This shows the importance of making full circumferential surveys rather than having a number of fixed rakes at several circumferential locations.

### Effect of Exit Rake Position on Radial Profiles of Exit Velocity

To determine if the previously discussed exit profiles at  $L/H = 6$  were fully developed, radial profiles of exit velocity were also measured at  $L/H = 2$ . Inlet conditions were held constant. The exit velocity profiles determined by the three nine-point pitot-static rakes are shown in figure 15 for the case of no suction and in figure 16 for a nominal suction of 10 percent, with approximately 6 percent suction on the outer wall and 4 percent on the inner wall. The inlet profiles are also shown. The profiles in figure 15(a) are typical of annular jets and indicate that the flow is separated from both walls at the  $L/H = 2$  position. At the  $L/H = 6$  position (fig. 15(b)) the flow has become attached to the inner wall, as shown by the strongly hub-weighted profiles. When a total suction rate of approximately 10 percent is applied, as shown in figure 16, the flow at  $L/H = 2$  (fig. 16(a)) is still detached from both walls, while the profiles at

$L/H = 6$  (fig. 16(b)) are again hub weighted. Comparing profiles with suction and without suction shows that profiles with suction are flatter at  $L/H$  of 2 or 6 due to the more effective flow spreading achieved with the suction-stabilized vortices.

#### Effect of Inlet Mach Number on Radial Profiles of Exit Velocity

Exit velocity profiles for nominal Mach numbers of 0.30, 0.34, and 0.40 are compared for the case of no suction in figure 17 and for a nominal suction rate of 7.5 percent in figure 18. The exit profiles shown in these figures were obtained by circumferentially averaging the results from the pitot-static exit rakes. As shown in figures 17 and 18, inlet Mach number has no effect on exit radial velocity profiles.

#### Diffuser Effectiveness

Diffuser effectiveness, as defined by equation (3), expresses the ratio of the actual to the ideal degree of conversion of dynamic pressure to static pressure between the diffuser inlet and exit stations. The effect of suction rate on diffuser effectiveness is shown in figure 4. For the best chamber geometry,  $x = 0.3 H$ ,  $y = 0.05 H$  (fig. 4(b)), the diffuser effectiveness increased from 48 percent without suction to 87 percent with 14.5 percent suction at an inlet Mach number of 0.18.

#### Circumferential Variation in Diffuser Effectiveness

From the circumferential surveys of exit velocity profiles, sufficient static pressure profile data were obtained to determine the local diffuser effectiveness values at each of the circumferential positions of the diffuser exit pitot-static rakes. As shown in figure 19 for a total suction rate of 10.2 percent, the circumferential variations in diffuser effectiveness values were less than 5 percent.

#### Diffuser Efficiency

The isentropic diffuser efficiency, as defined by equation (5), is a measure of total enthalpy conservation between diffuser inlet and exit stations. The relation between diffuser efficiency and diffuser total pressure loss is discussed in reference 9. Values of diffuser efficiency for the test conditions of this study are shown in tables I to IV.

## Diffuser Total Pressure Loss

The decrease in total pressure loss is shown in figure 20 for the range of inlet Mach numbers tested. For the case of no suction, the diffuser total pressure losses at inlet Mach numbers of 0.18 and 0.41 were 1.1 and 5.6 percent, respectively. For the same Mach numbers, the total pressure losses decreased to 0.48 and 5.2 percent at total suction rates of 14.4 and 5.6 percent, respectively. This reduction in total pressure loss is due to reductions in diffuser wall separation losses and in diffuser mass flow downstream of the suction gap. As shown in figure 21, when each of the five sets of total pressure loss data is normalized by the square of the particular inlet Mach number at which the data were obtained, the resulting values fall on a single curve. Thus, total pressure loss data obtained at low inlet Mach numbers can be extrapolated to inlet Mach numbers up to 0.41.

### Comparison of Performance of Two Short Dump Diffusers with Prediffuser Area Ratios of 1.15 and 1.40

The dump diffuser used in this investigation had also been used in a previous investigation, but with a prediffuser area ratio of 1.15 instead of 1.40. Table V compares some of the parameters measured in both tests. Both diffusers exhibited stable behavior to total suction rates of approximately 10 percent for the best  $x$  and  $y$  conditions and a Mach number of 0.18. For a total suction rate of 10.3 percent, the 1.40-area-ratio diffuser had an effectiveness of 75 percent, and the 1.15-area-ratio diffuser had an effectiveness of 87 percent. An effectiveness of 87 percent was obtained for the 1.40-area-ratio diffuser, but at a 14.5 percent suction rate. At this suction rate, the flow was not stable. The pressure loss was the same for both diffusers with no suction at inlet Mach numbers of 0.18 and 0.30. With no suction, the effectiveness values for the 1.15- and 1.40-area-ratio diffusers were approximately 40 and 48 percent, respectively.

## SUMMARY OF RESULTS

The performance of a short, annular suction-stabilized vortex diffuser with a variable vortex chamber and a prediffuser area ratio of 1.4 was evaluated in terms of diffuser velocity profiles, diffuser effectiveness, and total pressure loss for inlet Mach numbers of 0.18, 0.26, 0.30, 0.34, and 0.41. The test program consisted of a vortex-chamber-geometry screening phase followed by detailed performance evaluation of the

best vortex chamber geometry. The results are as follows:

1. The best chamber geometry based on diffuser effectiveness had inner- and outer-wall suction slots with a radial gap of 0.05 times and an axial gap of 0.3 times the prediffuser inlet height, respectively.

2. Diffuser effectiveness increased from 48 percent without suction to 87 percent at a 14.5 percent suction rate and an inlet Mach number of 0.18.

3. Diffuser total pressure loss at inlet Mach numbers of 0.18 and 0.41 decreased from 1.1 and 5.6 percent without suction to 0.48 and 5.2 percent at total suction rates of 14.4 and 5.6 percent, respectively.

4. At suction rates below 9 percent, with approximately 40 percent of the total suction applied on the inner wall and 60 percent on the outer wall, either hub- or tip-weighted radial profiles were maintained, depending on the profile existing without suction.

5. Radial profiles of exit velocity were invariant with inlet Mach number but they did change with suction rate. Radial profiles of exit velocity could be hub weighted by momentarily interrupting the outer-wall suction and tip weighted by momentarily interrupting the inner-wall suction.

6. The circumferential uniformity of radial profiles of inlet velocity deteriorated significantly as the total suction rate was increased above 10 percent. Above a suction rate of 10 percent, the radial profiles of exit velocity became circumferentially non-uniform, being made up of sectors containing hub-weighted, tip-weighted, and unstable profiles.

7. Comparing the performance of dump diffusers with prediffuser area ratios of 1.15 and 1.40, respectively, showed that both diffusers had stable flows to a total suction rate of about 10 percent. For the case of no suction, the 1.15- and 1.4-area-ratio diffusers for an exit rake position  $L/H$  of 6 had effectiveness values of 40 and 48 percent, respectively. Both diffusers had a best effectiveness of 87 percent. The 1.15-area-ratio diffuser achieved this value with a 10 percent total suction rate and stable flow; the 1.4-area-ratio diffuser required a 14 percent total suction rate and the flow was unstable. Inlet Mach number was 0.18 for both diffusers. For the 1.4-area-ratio diffuser with 10 percent total suction and stable flow, the effectiveness was 75 percent. This was 12 percent lower than the 1.15-area-ratio diffuser effectiveness for the same total suction rate.

Lewis Research Center,

National Aeronautics and Space Administration,

Cleveland, Ohio, December 1, 1977,

505-04.



## REFERENCES

1. Ringleb, Friedrich Otto: Flow Control by Generation of Standing Vortices and the Cusp Effect. Rept. 317, Princeton Univ., 1955.
2. Heskestad, Gunnar: Remarks on Snow Cornice Theory and Related Experiments with Sink Flows. J. Basic Eng., vol. 88, June 1966, pp. 539-549.
3. Heskestad, Gunnar: Further Experiments with Suction at a Sudden Enlargement in a Pipe. J. Basic Eng., vol. 92, Sept. 1970, pp. 437-449.
4. Juhasz, Albert J.: Performance of a Short Annular Dump Diffuser Using Wall Trailing Edge Suction. NASA TM X-3093, 1974.
5. Juhasz, Albert J.: Effect of Wall Edge Suction on the Performance of Short Annular Dump Diffuser with Exit Passage Flow Resistance. NASA TM X-3221, 1975.
6. Adkins, R. C.: A Short Diffuser with Low Pressure Loss. Fluid Mechanics of Combustion, J. L. Dussourd, R. P. Lohmann, and E. M. Uram, eds., Am. Soc. Mech. Eng., 1974, pp. 155-159.
7. Juhasz, Albert J.; and Smith, John M.: Performance of High-Area-Ratio Annular Dump Diffuser Using Suction-Stabilized-Vortex Flow Control. NASA TM X-3535, 1977.
8. Brighton, J. A.; and Jones, J. B.: Fully Developed Turbulent Flow in Annuli. J. Basic Eng., vol. 86, Dec. 1964, pp. 835-844.
9. Juhasz, Albert J.: Performance of an Asymmetric Short Annular Diffuser with a Nondiverging Inner Wall Using Suction. NASA TN D-7575, 1974.
10. Juhasz, Albert J.: Effect of Wall Suction on Performance of a Short Annular Diffuser at Inlet Mach Numbers up to 0.5. NASA TM X-3302, 1975.
11. Juhasz, Albert J.; and Holdeman, James D.: Preliminary Investigation of Diffuser Wall Bleed to Control Combustor Inlet Airflow Distribution. NASA TN D-6435, 1971.

TABLE I. - DIFFUSER PERFORMANCE DATA FOR AXIAL GAP OF 0.3 H

[Exit rake position, L/H, 6; inlet Mach number,  $M_1$ , 0.18.]

(a) Radial gap,  $y$ , -0.02 H

Diffuser inlet Mach number	Airflow		Inlet pressure				Inlet total temperature		Suction rate, percent			Diffuser effectiveness, $\eta$ , percent	Diffuser efficiency, $\epsilon$ , percent	Total pressure loss, $\Delta P_0/P_0$ , percent
	kg/sec	lbm/sec	Total		Static		K	$^{\circ}\text{F}$	Inner wall	Outer wall	Total			
			MPa	psia	MPa	psia								
0.182	2.30	5.08	$10.08 \times 10^{-2}$	14.62	$9.84 \times 10^{-2}$	14.27	276	36.4	0	0	0	47.9	52.4	1.10
.183	2.30	5.06	10.00	14.50	9.77	14.16		37.5	5.47	8.84	14.31	88.0	82.1	.42
.183	2.29	5.04	10.00	14.51	9.77	14.17		37.5	5.50	8.90	14.40	87.5	82.0	.42
.183	2.30	5.06	10.01	14.52	9.78	14.19		37.3	6.43	8.87	15.30	84.3	79.2	.48
.182	2.29	5.05	10.02	14.53	9.79	14.20		37.1	6.47	10.41	16.88	83.5	78.5	.50
.182	2.28	5.04	10.01	14.52	9.79	14.19		37.0	6.47	10.44	16.91	82.9	78.0	.51
.183	2.29	5.05	10.01	14.52	9.77	14.17		37.1	7.27	10.26	17.53	86.2	78.5	.50
.182	2.28	5.03	10.01	14.52	9.79	14.20		36.9	8.55	9.98	18.53	84.5	82.2	.41
.181	2.28	5.04	10.05	14.57	9.82	14.24		37.0	4.55	6.25	10.80	70.4	66.6	.76
.183	2.30	5.08	10.04	14.56	9.79	14.20		36.9	3.97	6.25	10.22	73.9	67.8	.75
.183	2.30	5.07	10.02	14.54	9.78	14.18		36.9	3.99	7.63	11.62	80.0	75.2	.58
.183	2.29	5.06	10.02	14.54	9.78	14.19		36.8	5.50	7.63	13.13	79.1	74.8	.58
.181	2.29	5.06	10.08	14.62	9.84	14.26		36.3	0	0	0	49.3	51.8	1.10
.183	2.28	5.04	9.94	14.42	9.69	14.06		37.4	0	0	0	48.8	50.9	1.14
.186	2.31	5.10	9.93	14.40	9.68	14.04		37.4	.73	1.49	2.22	52.8	54.5	1.09
.184	2.29	5.04	9.93	14.40	9.68	14.05		37.1	1.41	2.53	3.93	56.7	57.1	1.01
.185	2.30	5.06	9.92	14.38	9.68	14.03		37.1	2.11	3.67	5.78	59.9	58.4	.98
.183	2.27	5.00	9.90	14.36	9.67			36.9	2.88	5.26	8.14	67.6	63.1	.85
.183	2.27	5.01	9.91	14.37	9.67			36.9	2.33	5.18	7.51	65.9	64.2	.83
.184	2.28	5.03	9.91	14.37	9.67			36.8	3.75	5.50	9.25	68.0	62.6	.88
.183	2.27	5.00	9.90	14.35	9.66	14.00		36.8	4.03	6.19	10.21	73.3	65.2	.81
.184	2.27	5.01	9.87	14.32	9.64	13.98		36.8	5.52	8.73	14.26	88.6	82.0	.42



TABLE I. - Continued.

(c) Radial gap,  $y$ , 0.10 H

Diffuser inlet Mach number	Airflow		Inlet pressure				Inlet total temperature		Suction rate, percent			Diffuser effectiveness, $\eta$ , percent	Diffuser efficiency, $\epsilon$ , percent	Total pressure loss, $\Delta P_0/P_0$ , percent
	kg/sec	lbm/sec	Total		Static		K	$^{\circ}$ F	Inner wall	Outer wall	Total			
			MPa	psia	MPa	psia								
0.186	2.33	5.14	$9.98 \times 10^{-2}$	14.48	$9.73 \times 10^{-2}$	14.12	275	35.7	0	0	0	47.1	50.8	1.18
.185	2.31	5.09	9.98	14.47	9.73	14.12	276	36.7	0	0	0	48.0	51.2	1.15
.184	2.28	5.04	9.93	14.40	9.69	14.05		37.1	5.65	9.71	15.35	69.3	62.3	.88
.183	2.27	5.01	9.94	14.42	9.70	14.07		37.2	4.11	7.03	11.13	67.8	60.6	.91
.182	2.26	4.99	9.94	14.42	9.70	14.08		37.3	4.11	7.28	11.40	62.6	60.2	.91
.181	2.26	4.98	9.94	14.42	9.70	14.07		37.1	6.55	7.33	13.87	63.0	55.4	1.01
.181	2.26	4.99	9.96	14.45	9.72	14.10		37.4	0	6.77	6.77	49.5	52.4	1.08
.183	2.28	5.02	9.96	14.44	9.72	14.10		37.1	.87	1.98	2.85	53.7	55.8	1.02
.182	2.27	5.01	9.96	14.45	9.72	14.10		37.1	.87	1.90	2.77	50.1	53.5	1.07
.182	2.27	5.00	9.95	14.43	9.71	14.09		36.9	1.64	2.54	4.18	55.3	55.9	1.01
.184	2.30	5.07	9.96	14.44	9.72	14.09		37.1	1.52	2.40	3.92	52.1	51.6	1.14
.184	2.29	5.04	9.94	14.42	9.70	14.07		37.0	2.56	3.60	6.15	58.0	57.5	.99
.183	2.29	5.04	9.95	14.44	9.71	14.08		36.9	2.55	3.67	6.22	54.8	53.6	1.08
.182	2.27	5.00	9.94	14.42	9.71	14.08		36.9	2.97	4.51	7.48	58.6	58.0	.96
.183	2.28	5.03	9.95	14.43	9.71	14.08		36.9	2.92	4.59	7.51	57.4	54.9	1.05
.185	2.31	5.08	9.97	14.45	9.72	14.10		37.1	1.06	0	1.06	46.7	51.1	1.16
.182	2.30	5.06	10.10	14.65	9.84	14.27	277	38.0	0	0	0	47.5	48.7	1.17
.181	2.29	5.05	10.10	14.65	9.85	14.3	277	37.8	0	0	0	47.7	50.7	1.12
.181	2.79	5.04	10.07	14.61	9.83	14.65	276	37.5	4.07	6.24	10.31	63.3	55.8	1.01
.184	2.32	5.11	10.06	14.59	9.81	14.23		37.4	3.98	6.07	10.05	63.7	59.5	.95
.184	2.32	5.12	10.07	14.61	9.83	14.25		37.4	3.50	5.57	9.07	60.5	59.2	.96
.184	2.32	5.11	10.07	14.60	9.82	14.25		37.2	3.49	5.43	8.92	60.8	50.3	1.00
.182	2.29	5.05	10.07	14.61	9.83	14.30		36.9	1.57	2.70	4.27	54.9	55.6	1.01
.183	2.31	5.10	10.08	14.62	9.83	14.30		36.9	1.54	2.54	4.08	52.6	52.2	1.11
.183	2.31	5.09	10.07	14.61	9.83	14.25		36.6	2.82	5.46	8.28	56.2	54.3	1.05
.184	2.32	5.12	10.07	14.70	9.82	14.24		36.7	2.78	5.44	8.23	61.4	55.6	1.04
.183	2.30	5.08	10.06	14.58	9.82	14.24		36.5	4.53	7.55	12.08	66.9	61.6	.89
	2.30	5.07	10.06	14.59	9.82	14.24		36.5	4.42	7.53	11.96	63.5	59.9	.93
	2.31	5.09	10.06	14.59	9.81	14.23		36.3	5.53	7.51	13.04	65.2	59.1	.95
	2.30	5.08	10.05	14.58	9.81	14.23		36.4	5.56	8.74	14.29	72.7	66.7	.77
	2.31	5.10	10.06	14.59	9.81	14.23		36.4	6.47	8.76	15.23	71.0	64.2	.83
	2.30	5.07	10.06	14.59	9.82	14.25		36.3	7.45	8.79	16.24	66.1	60.5	.91
	2.31	5.09	10.06	14.59	9.82	14.25		36.3	8.29	8.74	17.03	65.6	58.7	.96
	2.31	5.09	10.09	14.64	9.85	14.30		36.4	.54	1.14	1.68	49.0	52.4	1.10
.184	2.33	5.13		14.63	9.84			36.4	1.78	2.79	4.57	55.2	56.3	1.03
.183	2.31	5.09		14.64				36.4	1.78	2.87	4.65	54.0	53.4	1.07
.184	2.32	5.12		14.63				36.3	2.30	3.46	5.77	55.2	53.9	1.08
.184	2.32	5.11	10.08	14.62				36.4	2.39	3.47	5.85	57.3	57.0	1.00
.248	3.11	6.85	10.18	14.76	9.74	14.13		36.1	1.77	2.57	4.34	53.8	57.0	1.81
.182	2.30	5.08	10.10	14.65	9.85	14.29		36.3	0	.70	.70	48.8	49.8	1.15
.183	2.32	5.11	10.10	14.64	9.85	14.29		36.3	0	1.44	1.44	51.6	55.1	1.04
.183	2.31	5.09	10.10	14.64	9.86	14.30		36.3	0	.87	.87	52.0	55.5	1.03

TABLE I. - Concluded.

(d) Radial gap,  $y$ , 0.15 H

Diffuser inlet Mach number	Airflow		Inlet pressure				Inlet total temperature		Suction rate, percent			Diffuser effectiveness, $\eta$ , percent	Diffuser efficiency, $\epsilon$ , percent	Total pressure loss, $\Delta P_0/P_0$ , percent
	kg/sec	lbm/sec	Total		Static		K	°F	Inner wall	Outer wall	Total			
			MPa	psia	MPa	psia								
0.184	2.30	5.08	$10.03 \times 10^{-2}$	14.55	$9.79 \times 10^{-2}$	14.19	277	38.9	1.17	0	1.17	47.3	51.4	1.13
.183	2.29	5.04	10.02	14.53	9.78	14.18		39.3	.5	0	.5	47.8	52.2	1.10
.181	2.26	4.99	10.02	14.53	9.78	14.18		39.4	.45	0	.45	47.6	51.6	1.09
		4.99	10.01	14.52	9.78	14.18		39.5	.89	1.60	2.49	49.0	52.5	1.07
		4.98	10.01	14.52	9.77	14.17		39.6	1.50	2.63	4.12	50.4	51.7	1.09
		4.98	10.00	14.51	9.77	14.17		39.6	2.24	3.78	6.02	52.5	53.9	1.04
.180	2.25	4.96	10.01	14.51	9.77	14.17		39.6	2.93	4.77	7.70	55.3	54.3	1.02
.180	2.24	4.95	10.00	14.50	9.76	14.16		39.5	3.23	5.59	8.82	56.4	54.8	1.01
.181	2.26	4.98	10.00	14.50	9.76	14.16		39.5	4.05	6.34	10.39	59.5	58.3	.94
.181	2.26	4.98	9.99	14.49	9.75	14.14		39.6	4.58	7.77	12.35	63.9	63.6	.83
.182	2.27	5.00	10.00	14.50	9.76	14.16			4.62	8.91	13.53	55.1	53.8	1.05
.181	2.26	4.98	9.98	14.48	9.74	14.13			5.59	8.93	14.53	60.4	56.4	.99
.182	2.27	5.01	9.98	14.47		14.12			6.45	8.95	15.40	65.2	62.5	.86
.182	2.26	4.99	9.97	14.47		14.12		39.4	6.13	8.97	15.10	62.0	57.2	.98
.182	2.27	5.01	9.98	14.47		14.12		39.3	6.52	9.04	15.55	64.1	64.4	.82
.184	2.27	5.01	9.91	14.37	9.66	14.01	278	41.3	0	0	0	46.2	51.0	1.15
.186	2.33	5.13	10.03	14.54	9.78	14.16		40.0	0	0	0	46.9	52.1	1.15
.181	2.26	4.99	10.02	14.53		14.19		40.7	.81	1.58	2.38	48.5	51.0	1.11
.183	2.29	5.05	10.03	14.54		14.19		40.8	.67	1.14	1.81	47.6	51.2	1.13
.183	2.29	5.04	10.02	14.54		14.18		40.9	1.35	2.44	3.79	50.0	51.2	1.13
.183	2.28	5.02	9.98	14.48	9.75	14.14		40.8	1.37	2.51	3.87	49.5	53.3	1.08
.182	2.27	5.01	10.01	14.52	9.77	14.17		40.5	2.44	3.73	6.17	52.2	51.4	1.11
.182	2.27	5.00			9.77	14.17		40.3	2.51	3.72	6.27	53.2	53.9	1.05
.183	2.29	5.04			9.77	14.17		40.2	2.98	5.22	8.20	52.4	53.7	1.07
.182	2.28	5.03			9.76	14.16		40.0	2.98	5.26	8.24	55.1	51.2	1.12
.183	2.29	5.05		14.51				40.0	3.55	5.53	9.08	53.9	55.0	1.05
.182	2.28	5.02		14.52				39.8	3.54	5.51	9.05	54.9	51.7	1.11
.182	2.28	5.02		14.52				39.9	4.00	6.18	10.18	56.8	52.7	1.09
.183	2.29	5.06		14.51				39.6	3.97	6.10	10.07	55.2	53.5	1.08
.183	2.29	5.04	10.00	14.51				39.6	4.54	6.45	10.98	56.5	54.1	1.06
.182	2.28	5.03		14.51		14.15	277	39.5	4.53	6.44	10.97	57.2	52.7	1.07
.183	2.28	5.03		14.50	9.74	14.13		39.5	4.51	7.56	12.08	61.8	55.7	1.02
.184	2.29	5.06		14.50	9.75	14.15		39.4	4.59	7.46	12.04	56.4	54.9	1.05
.183	2.29	5.06		14.51	9.76	14.15		39.2	4.42	8.70	14.12	56.6	52.1	1.12
.184	2.20	5.06		14.50	9.74	14.13		39.1	5.52	8.79	14.31	64.4	57.5	.99
.183	2.28	5.03		14.50	9.76	14.15		39.2	6.42	8.86	15.28	61.4	57.2	.99
.183	2.29	5.05		14.50	9.76	14.15		39.1	6.41	8.83	15.25	61.7	57.8	.98
.184	2.30	5.06		14.51	9.75	14.14		38.9	7.36	8.80	16.16	61.1	55.4	1.04
.184	2.30	5.07	10.01	14.51	9.76	14.16		38.9	4.57	8.57	13.14	53.9	52.7	1.11
.183	2.30	5.06	10.02	14.54	9.78	14.18		38.7	0	0	0	47.5	50.5	1.15

TABLE II. - DIFFUSER PERFORMANCE FOR AXIAL GAPS OF 0.2 H AND 0.4 H

[Exit rake position, L/H, 6; inlet Mach number,  $M_1$ , 0.18.]

(a) Axial gap, x, 0.2 H; radial gap, y, 0.05 H

Diffuser inlet Mach number	Airflow		Inlet pressure				Inlet total temperature		Suction rate, percent			Diffuser effectiveness, $\eta$ , percent	Diffuser efficiency, $\epsilon$ , percent	Total pressure loss, $\Delta P_0/P_0$ , percent
	kg/sec	lbm/sec	Total		Static		K	$^{\circ}\text{F}$	Inner wall	Outer wall	Total			
			MPa	psia	MPa	psia								
0.182	2.28	5.03	$10.04 \times 10^{-2}$	14.56	$9.78 \times 10^{-2}$	14.19	278	40.4	0	0	0	47.5	49.9	1.15
↓	2.29	5.04	10.03	14.54	9.79	14.19	278	39.9	0	0	0	47.9	51.1	1.13
↓	2.27	5.01	10.00	14.50	9.76	14.16	277	39.0	2.69	6.33	9.02	58.1	57.6	.97
↓	2.27	5.00	9.99	14.49	9.75	14.14	↓	38.7	4.07	6.34	10.41	67.9	64.6	.81
.181	2.26	4.98	9.99	14.48	9.75	14.15	↓	38.6	4.41	8.79	13.19	68.0	64.9	.79
.182	2.27	5.01	9.98	14.47	9.75	14.14	↓	38.6	5.56	8.81	14.37	73.3	70.2	.69
.181	2.26	4.98	9.98	14.48	9.74	14.13	276	38.4	6.62	8.70	15.31	72.0	67.6	.73
.183	2.28	5.04	9.98	14.48	9.73	14.12	278	40.5	0	0	0	47.1	50.0	1.17
.184	2.29	5.04	9.97	14.46	9.72	14.10	277	39.1	.76	1.52	2.28	51.3	52.9	1.10
.183	2.28	5.03	9.97	14.45	9.72	14.00	↓	38.9	1.50	2.56	4.06	53.7	51.7	1.12
.184	2.28	5.03	9.95	14.43	9.71	14.08	↓	38.7	1.75	3.72	5.47	56.1	57.0	1.00
.184	2.29	5.05	9.96	14.44	↓	↓	↓	38.6	1.75	3.79	5.53	59.2	56.5	1.02
.185	2.30	5.07	9.95	14.43	↓	↓	↓	38.6	2.48	4.69	7.17	60.9	59.8	.95
.184	2.29	5.05	9.95	14.43	↓	↓	↓	38.6	2.48	4.71	7.19	59.3	59.5	.95
.185	2.29	5.06	9.94	14.42	↓	↓	↓	38.5	3.01	5.59	8.60	61.5	62.7	.88
.183	2.27	5.01	↓	↓	9.69	14.06	↓	38.5	3.02	5.66	8.68	66.3	60.6	.91
.185	2.30	5.07	↓	↓	9.70	14.07	↓	38.5	3.23	6.27	9.51	63.4	61.8	.91
.185	2.30	5.07	↓	↓	9.70	14.07	↓	38.6	4.00	6.27	10.27	65.5	63.2	.87
.184	2.29	5.09	↓	14.41	9.71	14.08	↓	38.5	4.05	7.69	11.73	65.3	64.2	.84
.184	2.29	5.09	9.93	14.41	9.69	14.06	↓	38.6	4.05	7.70	11.75	70.4	65.8	.80
.184	2.29	5.05	9.93	14.41	9.68	14.04	↓	38.7	4.49	7.69	12.17	72.1	66.5	.79
.185	2.30	5.06	9.94	14.42	9.70	14.08	↓	38.9	2.07	3.62	5.69	60.6	61.5	.91
.185	2.29	5.04	9.92	14.39	9.68	14.04	↓	38.8	5.58	8.88	14.46	76.5	70.6	.69
.184	2.29	5.04	9.93	14.40	9.67	14.03	↓	38.8	6.49	8.88	15.38	74.6	68.6	.74
.185	2.30	5.06	9.93	14.40	9.67	14.03	↓	38.9	7.44	8.86	16.31	71.9	67.6	.77
↓	2.29	5.05	9.93	14.40	9.68	14.04	↓	38.9	8.38	8.95	17.33	72.1	66.6	.79
↓	2.30	5.06	9.94	14.42	9.70	14.08	↓	38.9	2.07	3.62	5.69	60.6	61.54	.91
↓	2.31	5.08	9.95	14.44	9.70	14.07	↓	39.0	2.06	3.65	5.71	58.0	56.27	1.04
.184	2.29	5.04	9.92	14.38	9.68	14.04	↓	39.0	5.51	10.65	16.17	76.9	71.83	.66
.185	↓	↓	9.91	14.37	9.68	14.03	↓	39.2	6.52	10.67	17.20	80.5	76.07	.57
.185	↓	↓	9.91	14.37	9.70	14.07	↓	39.1	7.42	10.68	18.10	77.4	78.76	.50
.184	↓	↓	9.92	14.39	9.67	14.03	↓	39.1	8.35	10.62	18.97	75.5	69.15	.73
.185	2.30	5.07	9.94	14.42	9.71	14.08	↓	39.1	2.19	3.94	6.13	60.0	60.71	.93
.184	2.28	5.03	9.94	14.42	9.70	14.07	↓	39.2	2.18	4.05	6.23	58.6	55.75	1.03



TABLE III. - DIFFUSER PERFORMANCE DATA FOR SEVERAL INLET MACH NUMBERS

[Axial gap, x, 0.3 H; radial gap, y, 0.05 H; exit rake position, L/H, 6.]

(a) Inlet Mach number,  $M_1$ , 0.26

Diffuser inlet Mach number	Airflow		Inlet pressure				Inlet total temperature		Suction rate, percent			Diffuser effectiveness, $\eta$ , percent	Diffuser efficiency, $\epsilon$ , percent	Total pressure loss, $\Delta P_0/P_0$ , percent
	kg/sec	lbm/sec	Total		Static		K	°F	Inner wall	Outer wall	Total			
			MPa	psia	MPa	psia								
0.249	3.08	6.78	$10.11 \times 10^{-2}$	14.67	$9.66 \times 10^{-2}$	14.01	281	45.6	0	0	0	47.2	52.0	2.04
.251	3.10	6.84	10.10	14.64	9.63	13.97	279	42.4	.94	1.82	2.76	52.5	54.7	1.96
.252	3.11	6.85	10.08	14.62	9.62	13.96	279	41.9	1.57	2.56	4.13	55.5	58.4	1.81
.252	3.11	6.85	10.07	14.61	9.62	13.95	278	41.0	2.52	3.90	6.42	59.8	61.1	1.69
.260	3.23	7.12	10.13	14.69	9.64	13.92	278	40.1	0	0	0	47.3	52.3	2.22
.259	3.19	7.04	10.06	14.59	9.57	13.88	277	39.3	4.16	5.81	9.97	65.0	62.0	1.75
.258	3.19	7.03	10.07	14.60	9.58	13.90	277	39.0	3.49	5.83	9.32	65.2	63.3	1.68
.260	3.20	7.06	10.06	14.59	9.58	13.89	277	39.4	4.85	5.80	10.65	63.4	61.3	1.79
↓	3.20	7.05	10.05	14.57	9.55	13.85	277	38.9	4.86	7.20	12.06	71.3	65.9	1.58
↓	3.20	7.05	10.04	14.56	9.55	13.85	277	39.5	4.11	7.19	11.30	73.0	67.3	1.52
↓	3.19	7.04	10.04	14.56	9.56	13.87	277	39.5	4.45	7.19	11.64	70.6	66.4	1.56
.258	3.18	7.02	10.05	14.58	9.57	13.88	277	39.0	5.28	7.23	12.50	69.9	64.6	1.62
.250	3.09	6.81	10.05	14.58	9.60	13.93	277	40.6	3.37	5.47	8.85	64.7	61.7	1.65
.260	3.20	7.06	10.08	14.62	9.58	13.90	278	39.7	4.13	4.83	8.96	61.1	58.5	1.92
.261	3.22	7.10	10.07	14.60	9.57	13.89	277	39.0	4.12	5.35	9.47	62.2	60.0	1.87
.261	3.21	7.07	10.05	14.57	9.57	13.87	277	39.5	5.44	7.17	12.61	69.1	64.0	1.68
.259	3.19	7.04	10.05	14.58	9.57	13.87	277	39.3	5.46	7.19	12.62	69.3	64.0	1.66
.260	3.20	7.06	10.06	14.59	9.58	13.90	277	39.2	3.46	7.14	10.61	63.8	63.1	1.71
.249	3.06	6.76	10.03	14.55	9.60	13.92	279	41.6	4.22	6.53	10.75	68.1	68.3	1.35
.251	3.09	6.92	10.05	14.57	9.60	13.92	279	41.5	3.29	5.58	8.87	64.6	64.9	1.52
.261	3.09	6.81	10.05	14.58	9.61	13.94	278	41.0	3.83	5.56	9.39	67.2	67.2	1.42

(b) Inlet Mach number,  $M_1$ , 0.30

0.298	3.66	8.08	$10.21 \times 10^{-2}$	14.81	$9.57 \times 10^{-2}$	13.89	280	44.5	0	0	0	47.0	51.0	2.97
.296	3.64	8.02	10.19	14.78	9.55	13.86	279	42.2	.79	1.46	2.25	50.6	52.7	2.82
.297	3.65	8.05	10.18	14.77	9.54	13.84	278	40.9	1.34	2.18	3.52	53.0	54.6	2.73
.295	3.63	8.00	10.17	14.74	9.53	13.82	278	40.5	2.15	3.33	5.47	56.5	55.9	2.62
.298	3.66	8.06	10.16	14.74	9.52	13.80	278	40.1	2.46	3.70	6.16	58.2	58.6	2.50
.299	3.66	8.08	10.15	14.72	9.51	13.79	277	40.0	2.83	4.65	7.48	60.7	60.4	2.41
.316	3.87	8.53	10.18	14.77	9.47	13.74	277	39.0	2.77	4.00	6.77	58.8	58.8	2.79
.311	3.81	8.39	10.18	14.76	9.49	13.77	277	38.9	2.81	4.07	6.89	58.4	59.2	2.67
.309	3.78	8.34	10.16	14.74	9.48	13.75	277	38.8	3.47	4.54	8.02	59.5	59.6	2.62
.305	3.74	8.24	10.15	14.72		13.75	277	38.9	3.54	4.95	8.49	61.5	60.1	2.53
.306	3.75	8.27	10.16	14.73		13.75	277	38.6	2.95	4.95	7.90	62.3	60.8	2.52
.305	3.74	8.24	10.15	14.72		13.75	277	38.9	4.13	4.96	9.09	60.2	59.9	2.54
.304	3.71	8.19	10.14	14.70	9.46	13.72	277	38.8	4.14	6.16	10.3	64.4	60.8	2.46
.306	3.74	8.25	10.14	14.70	9.47	13.74	277	38.9	3.50	6.11	9.61	65.4	62.1	2.41
.305	3.73	8.23	10.14	14.71	9.50	13.78	277	38.8	2.95	6.08	9.03	59.6	61.2	2.46
.305	3.72	8.21	10.13	14.69	9.47	13.74	277	39.0	3.80	6.14	9.94	64.8	63.1	2.33
.303	3.71	8.17	10.14	14.70	9.48	13.75	277	38.9	4.51	6.17	10.68	64.2	62.6	2.34
.306	3.74	8.24	10.14	14.71	9.48	13.75	277	39.1	4.64	6.11	10.75	63.2	60.7	2.50
.299	3.63	8.01	10.03	14.54	9.38	13.61	276	36.2	4.89	6.54	11.43	56.6	57.4	2.59
.303	3.73	8.23	10.23	14.84	9.56	13.87	278	41.4	0	0	0	47.64	50.26	3.10
.304	3.71	8.17	10.10	14.65	9.41	13.65	278	39.9	3.79	6.38	10.17	65.9	62.2	2.39



TABLE III. - Concluded.

(c) Inlet Mach number,  $M_1$ , 0.34

Diffuser inlet Mach number	Airflow		Inlet pressure				Inlet total temperature		Suction rate, percent			Diffuser effectiveness, $\eta$ , percent	Diffuser efficiency, $\epsilon$ , percent	Total pressure loss, $\Delta P_0/P_0$ , percent
	kg/sec	lbm/sec	Total MPa	Static		K	$^{\circ}\text{F}$	Inner wall	Outer wall	Total				
				psia	MPa						psia			
0.342	4.21	9.28	$10.35 \times 10^{-2}$	15.01	$9.45 \times 10^{-2}$	13.71	277	39.5	0.44	1.30	1.74	51.6	49.1	4.01
.347	4.27	9.41	10.36	15.03	9.43	13.68		39.2	.44	1.26	1.71	51.6	48.9	4.14
.348	4.25	9.38	10.31	14.95	9.42	13.66		39.4	1.92	4.77	6.70	52.8	54.6	3.70
.348	4.25	9.38	10.29	14.93	9.39	13.62		39.3	2.48	4.80	7.28	55.8	55.9	3.60
.347	4.23	9.33	10.27	14.90	9.37	13.60		39.2	3.01	4.81	7.82	59.8	58.4	3.38
.346	4.23	9.33	10.28	14.92	9.38	13.61		39.1	2.99	4.74	7.72	60.9	56.9	3.48
.347	4.24	9.35	10.29	14.93	9.38	13.61		38.9	3.50	4.76	8.26	59.9	56.1	3.56
.350	4.27	9.40	10.28	14.92	9.36	13.58		39.0	3.48	5.51	8.99	62.7	58.0	3.46
.349	4.25	9.37	10.26	14.89	9.36	13.58		39.0	3.47	5.46	8.92	62.8	60.2	3.27
.351	4.28	9.43	10.28	14.91	9.36	13.58		38.8	4.03	5.55	9.58	62.9	58.8	3.42
.343	4.20	9.26	10.29	14.92	9.38	13.60		38.6	4.60	5.66	10.26	61.8	55.3	3.55
.347	4.27	9.41	10.34	15.00	9.45	13.71		38.7	0	1.28	1.28	49.5	53.1	3.81
.342	4.22	9.30	10.35	15.02	9.46	13.73		38.4	0	1.30	1.30	51.2	50.5	3.91
.344	4.24	9.35	10.36	15.03	9.46	13.73		38.5	.66	1.31	1.98	51.1	49.9	3.99
.345	4.25	9.38	10.36	15.03	9.45	13.71		38.6	.80	1.41	2.21	51.2	49.5	4.05
.346	4.27	9.40	10.36	15.03	9.44	13.70		38.6	1.01	1.68	2.69	52.0	50.3	4.02
.346	4.25	9.38	10.34	15.00	9.43	13.67		38.5	1.04	2.01	3.05	53.6	52.0	3.87
.345	4.24	9.36	10.34	15.00	9.42	13.66		38.3	1.55	2.52	4.07	54.5	51.2	3.92
.348	4.26	9.40	10.31	14.95	9.43	13.67		38.4	1.69	3.36	5.06	54.0	55.7	3.62
.347	4.24	9.35	10.29	14.92	9.40	13.64		38.5	2.15	3.37	5.52	56.7	56.6	3.52
.346	4.25	9.37	10.32	14.97	9.40	13.63		38.3	2.13	3.42	5.55	57.4	54.9	3.65
.347	4.25	9.37	10.30	14.93	9.41	13.65		38.5	2.16	4.14	6.29	54.6	56.1	3.57
.349	4.26	9.39	10.29	14.93	9.39	13.62		38.4	2.42	4.17	6.59	59.8	57.8	3.46
.347	4.25	9.39	10.30	14.94	9.39	13.61		38.4	3.04	4.14	7.17	59.2	55.1	3.65
.344	4.25	9.39	10.29	15.06	9.48	13.75		38.5	0	0	0	47.7	48.1	4.13

(d) Inlet Mach number,  $M_1$ , 0.41

0.403	4.87	10.73	$10.44 \times 10^{-2}$	15.14	$9.21 \times 10^{-2}$	13.35	278	41.2	0.67	1.18	1.85	50.26	48.0	5.62
.406			10.39	15.07	9.16	13.28		41.2	1.21	2.79	4.00	55.0	52.4	5.21
.405			10.40	15.08	9.16	13.28		41.2	1.58	2.66	4.24	54.8	52.4	5.20
			10.40	15.08	9.16	13.28		41.3	2.10	2.88	4.98	54.4	50.6	5.38
	4.86	10.72	10.40	15.08	9.15	13.27		41.3	2.10	3.06	5.16	54.7	50.3	5.42
	4.86	10.72	10.39	15.07	9.15	13.27		41.0	2.10	3.25	5.35	55.6	52.2	5.21
	4.87	10.73	10.40	15.08	9.16	13.29		41.2	1.59	2.69	4.28	54.0	51.1	5.33
.404	4.87	10.73	10.43	15.13	9.18	13.32		41.2	1.01	1.73	2.74	51.5	49.2	5.54
.403	4.86	10.72	10.43	15.13	9.19	13.33		41.2	.66	1.62	2.29	51.6	49.2	5.49
.402	4.86	10.72	10.43	15.13	9.21	13.36		41.2	.66	1.27	1.93	50.6	48.9	5.50
.401	4.86	10.72	10.45	15.16	9.24	13.40		41.3	0	0	0	48.1	47.3	5.63
.402	4.89	10.79	10.49	15.22	9.27	13.45	277	38.2	0	0	0	46.4	47.7	5.60
.403		10.78	10.46	15.18	9.24	13.41		38.0	.64	1.14	1.79	49.3	49.4	5.46
.404		10.78	10.44	15.14	9.23	13.38		38.1	1.03	1.69	2.71	50.8	50.6	5.36
.403		10.79	10.46	15.17	9.22	13.37		38.0	.74	1.69	2.43	50.7	49.3	5.48
.404		10.79	10.44	15.14	9.21	13.35		37.9	1.15	2.10	3.25	52.0	50.5	5.37
.405		10.78	10.42	15.12	9.19	13.33		38.0	1.39	2.55	3.94	53.5	51.4	5.30
.405	4.90	10.79	10.43	15.12	9.19	13.33		38.1	1.83	2.86	4.69	53.5	51.3	5.31
.405	4.89	10.78	10.45	15.10	9.18	13.32		38.0	2.11	3.27	5.38	55.2	52.3	5.20
.406	4.89	10.79	10.40	15.09	9.16	13.29			2.10	3.50	5.60	56.2	52.8	5.17
.406	4.89	10.79	10.41	15.10	9.17	13.29			1.86	3.57	5.44	56.0	52.7	5.17
.405	4.90	10.80	10.42	15.12	9.17	13.30			1.86	3.21	5.07	55.2	51.2	5.33

TABLE IV. - DIFFUSER PERFORMANCE FOR CIRCUMFERENTIAL SURVEY

[Axial gap, x, 0.3 H; radial gap, y, 0.05 H; exit rake position, L/H, 6; inlet Mach number,  $M_1$ , 0.18.]

(a) Total suction rate,  $S_t$ , 10.2 percent

Circumferential position, deg	Diffuser inlet Mach number	Airflow		Inlet pressure				Inlet total temperature		Suction rate, percent			Diffuser effectiveness, $\eta$ , percent	Diffuser efficiency, $\epsilon$ , percent	Total pressure loss, $\Delta P_0/P_0$ , percent
		kg/sec	lbm/sec	Total		Static		K	$^{\circ}$ F	Inner wall	Outer wall	Total			
				MPa	psia	MPa	psia								
0	0.185	2.28	5.03	$9.92 \times 10^{-2}$	14.39	$9.67 \times 10^{-2}$	14.03	280	44.7	3.93	6.17	10.10	69.0	66.0	0.81
10	.185	2.28	5.03	↓	↓	9.67	14.03	↓	44.3	3.94	6.16	10.10	69.8	69.9	.71
20	.184	2.27	5.01	↓	↓	9.68	14.05	↓	44.3	3.96	6.17	10.13	69.4	70.2	.70
30	.184	2.27	5.01	↓	↓	↓	14.04	↓	44.0	3.95	6.23	10.18	70.8	67.3	.77
40	.186	2.29	5.06	↓	↓	↓	14.04	↓	44.0	3.94	6.22	10.16	70.5	67.5	.78
50	.185	2.28	5.03	↓	↓	↓	14.04	↓	44.0	3.95	6.19	10.14	69.4	67.0	.78
60	.184	2.27	5.00	↓	↓	↓	14.03	↓	43.9	3.98	6.15	10.13	70.3	64.9	.82
70	↓	↓	5.01	↓	↓	↓	14.04	↓	44.0	3.96	6.19	10.15	69.6	61.4	.91
70	↓	↓	5.00	↓	↓	↓	14.04	↓	43.9	4.00	6.27	10.27	68.9	61.1	.91
80	↓	↓	5.00	↓	↓	9.69	14.05	↓	43.8	3.97	6.26	10.22	67.7	63.0	.87
90	↓	↓	4.99	↓	↓	9.67	14.03	↓	43.9	3.98	6.21	10.19	70.2	66.2	.79
100	.185	2.28	5.04	↓	↓	9.67	14.03	↓	43.9	3.97	6.14	10.11	70.8	67.3	.78
110	.184	2.27	5.00	9.93	14.40	9.68	14.03	↓	43.8	3.96	6.22	10.18	70.0	68.0	.75
120	.184	2.27	5.00	9.92	14.39	9.68	14.04	↓	43.9	3.99	6.25	10.24	70.8	69.0	.73

(b) Total suction rate,  $S_t$ , 14.4 percent

0	0.182	2.27	5.00	$9.96 \times 10^{-2}$	14.45	$9.72 \times 10^{-2}$	14.10	278	40.3	5.36	9.07	14.43	83.4	78.9	0.56
10	.182	2.26	4.99	9.97	14.46	9.72	14.10	↓	40.2	5.36	9.10	14.45	83.4	74.1	.59
20	.180	2.24	4.94	↓	↓	9.72	14.10	↓	40.2	5.39	9.14	14.52	82.9	73.4	.60
30	.181	2.26	4.98	↓	↓	9.73	14.11	↓	40.2	5.38	9.08	14.46	82.4	71.9	.64
40	.182	2.27	5.00	↓	↓	9.72	14.10	↓	40.3	5.32	9.05	14.37	83.0	74.0	.60
50	↓	↓	5.01	↓	↓	↓	14.09	↓	40.4	5.33	9.06	14.38	82.7	74.0	.60
60	↓	↓	5.01	↓	↓	↓	14.10	↓	40.3	5.34	9.05	14.39	81.9	73.3	.61
70	↓	↓	5.00	9.96	14.45	↓	14.10	↓	40.2	5.34	9.02	14.36	85.0	76.5	.54
80	↓	2.27	4.99	9.97	14.46	↓	14.09	↓	40.2	5.35	9.07	14.43	82.4	73.8	.60
90	↓	2.26	4.99	↓	↓	9.71	14.08	↓	40.4	5.36	9.07	14.43	83.3	73.1	.62
100	↓	2.27	5.01	↓	↓	9.72	14.10	↓	40.3	5.34	9.03	14.37	84.0	74.8	.58
110	.183	2.27	5.01	↓	↓	9.73	14.11	↓	40.3	5.32	8.98	14.30	84.2	77.6	.57
120	.182	2.26	4.99	↓	↓	9.72	14.10	↓	40.2	5.33	9.03	14.36	81.9	72.9	.62

TABLE V. - COMPARISON OF DIFFUSERS WITH PREDIFFUSER

AREA RATIOS OF 1.15 AND 1.4

[Exit rake position, L/H, 6; best effectiveness,  $\eta$ , ~ 87 percent.]

Prediffuser area ratio	Best axial gap, <sup>a</sup> x	Best radial gap, <sup>a</sup> y	Best suction rate, percent	Pressure loss, <sup>b</sup> $\Delta P_0/P_0$ , percent	Pressure loss with no suction, at Mach -		Effectiveness with no suction, $\eta$ , percent
					0.18	0.30	
1.15	0.45 H	0.15 H	10.3	0.45	1.20	3.15	~40
1.40	.30 H	.05 H	14.5	.44	1.10	3.10	~48

<sup>a</sup>Diffuser inlet passage height, H, 2.54 cm.

<sup>b</sup>Inlet Mach number,  $M_1$ , 0.18.

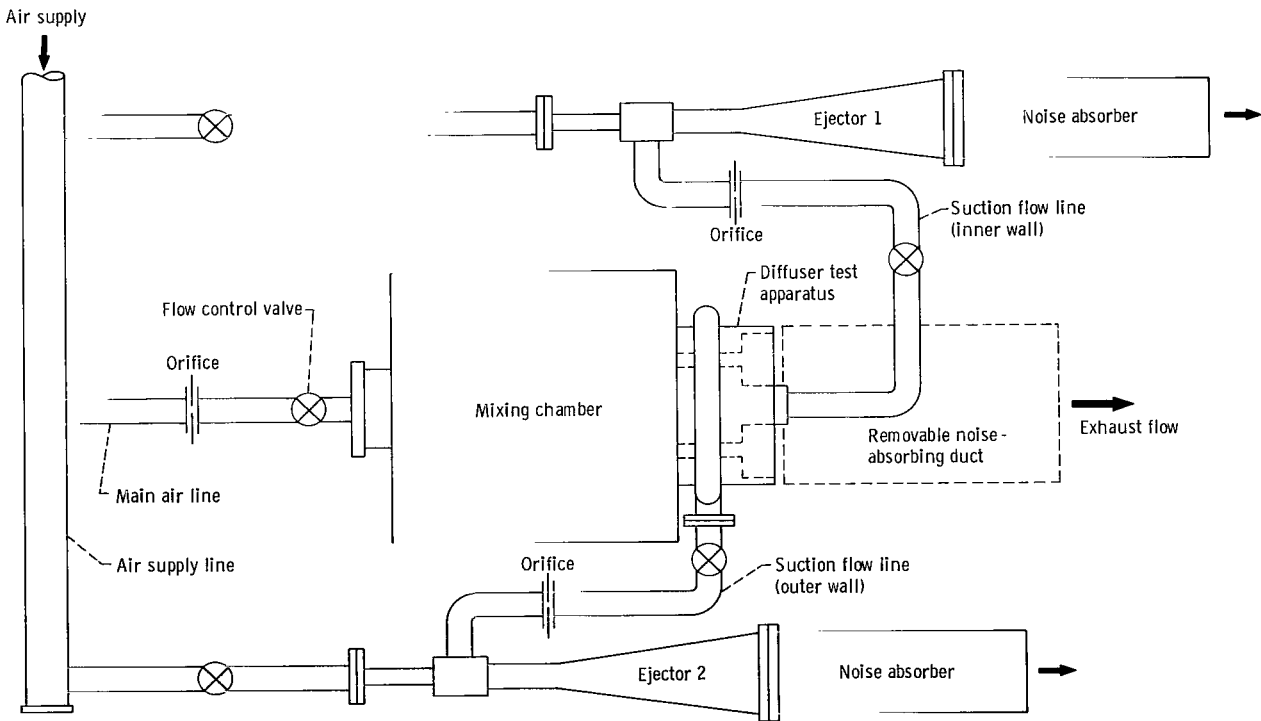


Figure 1. - Test facility flow system.

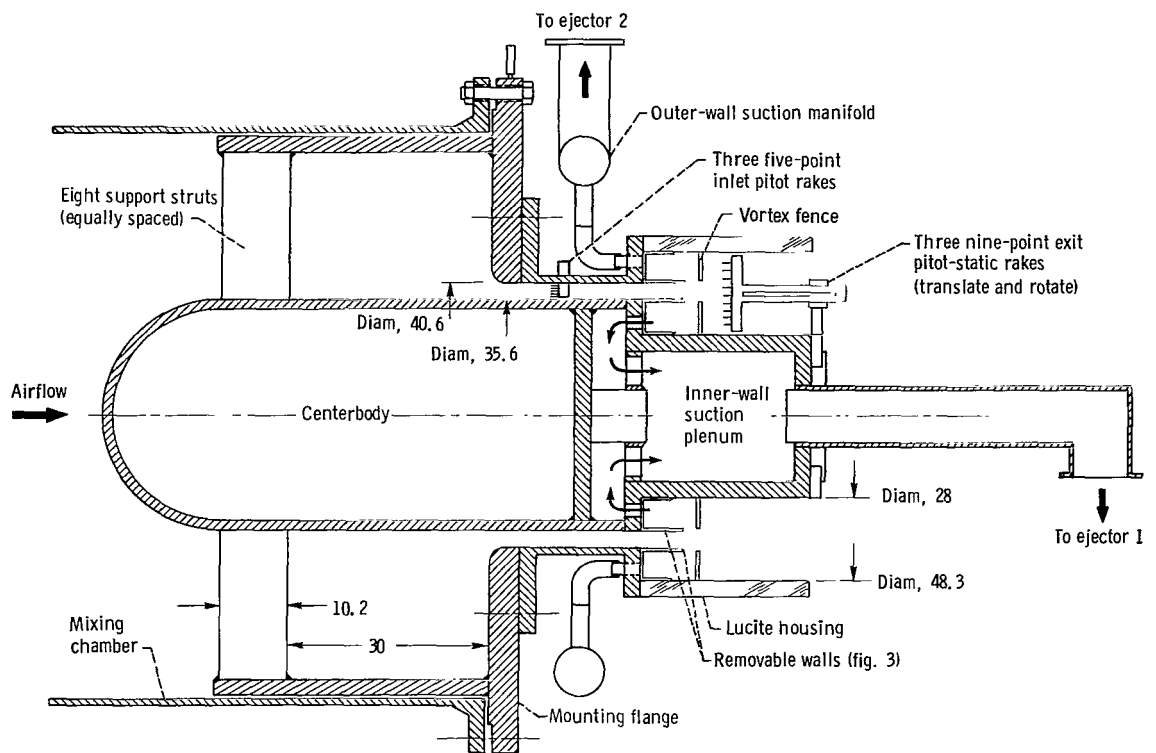


Figure 2. - Cross section of annular diffuser test apparatus. (Dimensions are in cm.)

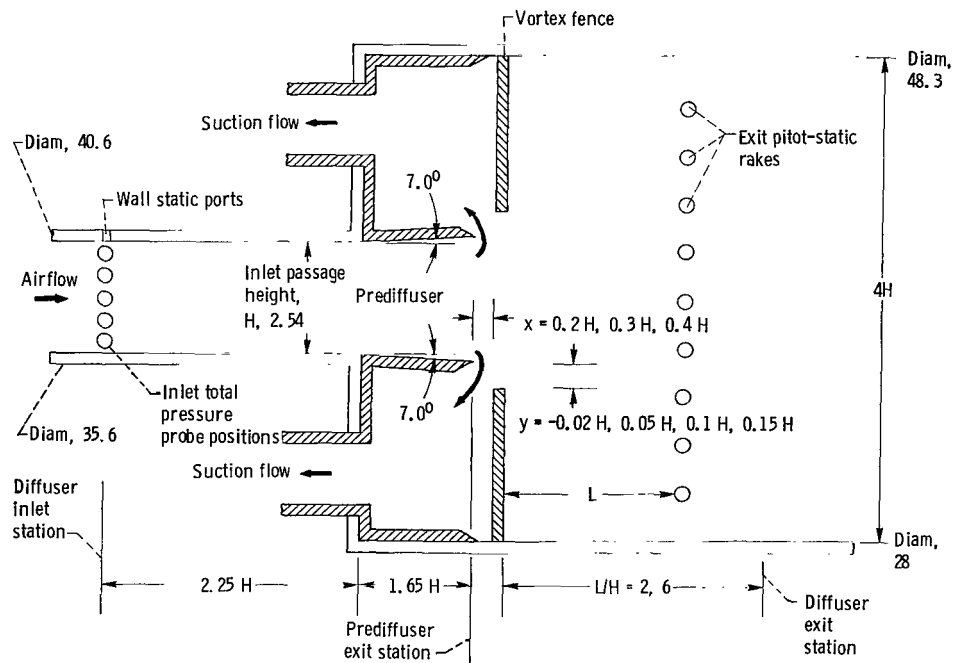


Figure 3. - Details of diffuser annulus passage. (Dimensions are in cm.)

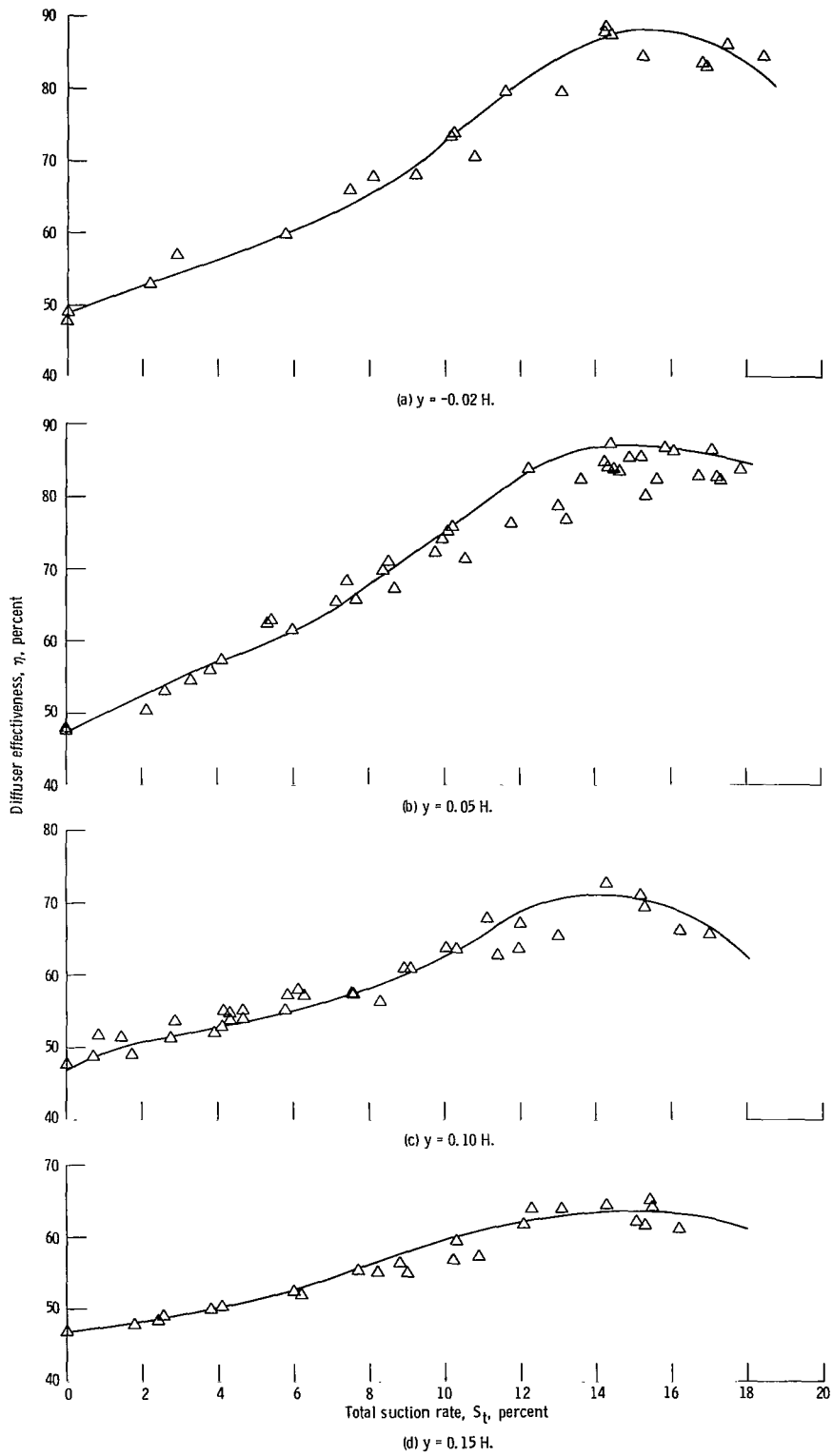


Figure 4. - Effect of changing radial gap  $y$  on diffuser effectiveness for a fixed axial gap  $x$  of  $0.3 H$  over a range of total suction rates. Exit rake position,  $L/H$ , 6; diffuser inlet height,  $H$ , 2.54 centimeters; inlet Mach number,  $M_1$ , 0.18.

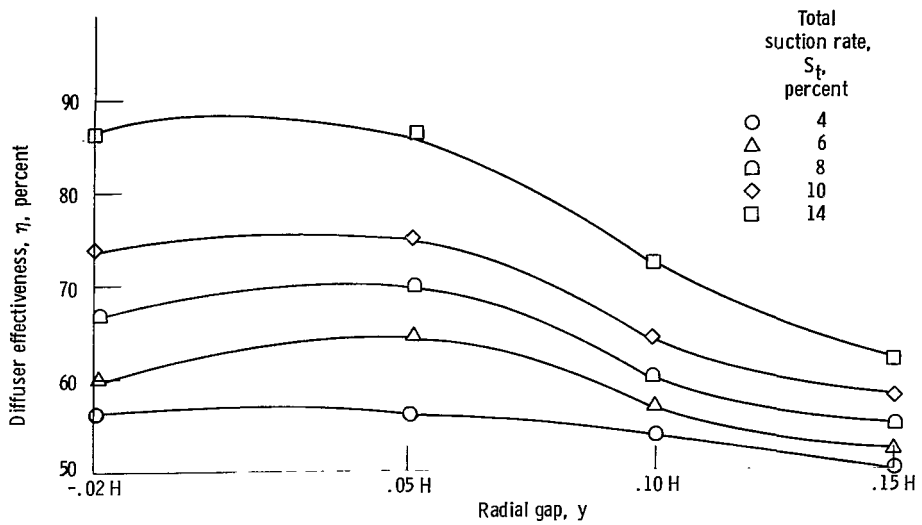


Figure 5. - Effect of changing radial gap  $y$  on diffuser effectiveness for a fixed axial gap  $x$  of  $0.3 H$  for five fixed suction rates. Exit rake position,  $L/H$ , 6; diffuser inlet height,  $H$ , 2.54 centimeters; inlet Mach number,  $M_1$ , 0.18.

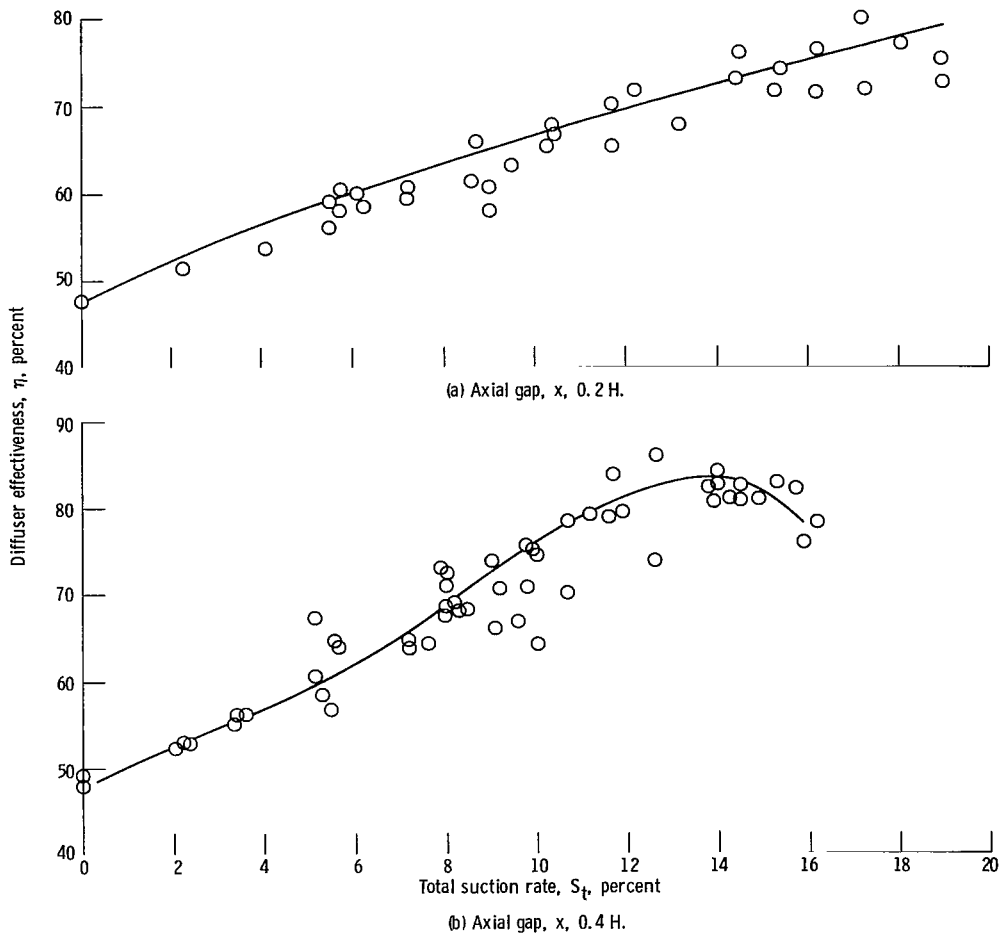


Figure 6. - Effect of suction rate on diffuser effectiveness for a fixed radial gap  $y$  of 0.05 H and two values of axial gap  $x$ . Exit rake position,  $L/H$ , 6; diffuser inlet height,  $x$ , 2.54 centimeters; inlet Mach number,  $M_1$ , 0.18.

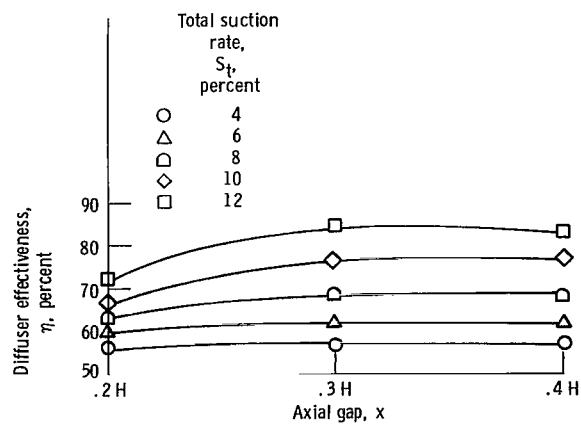
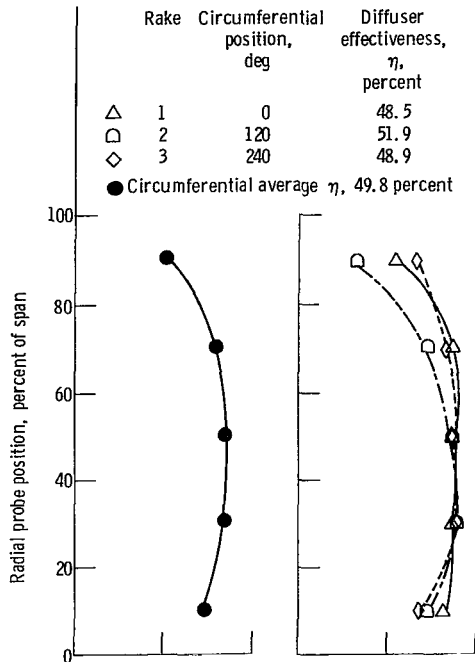
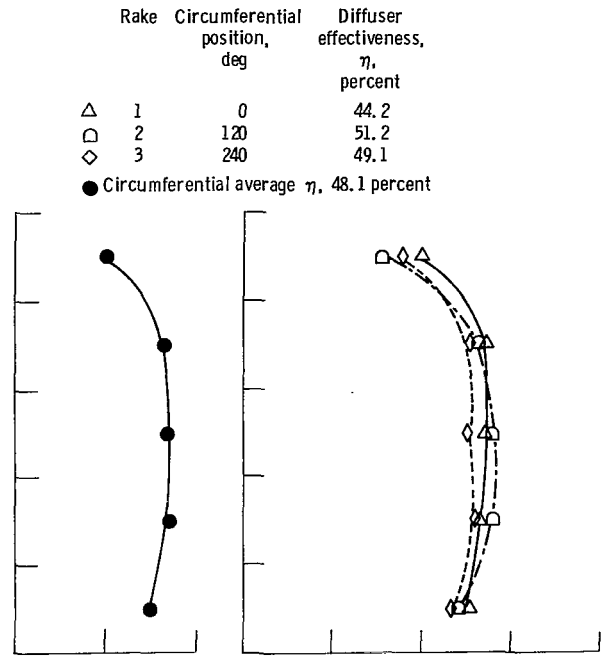


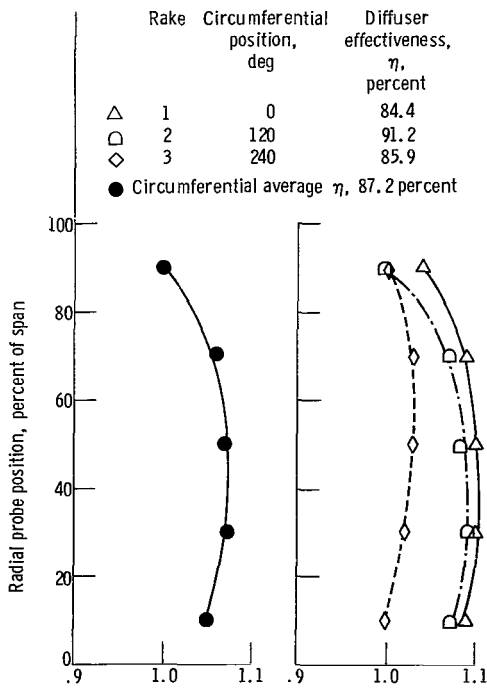
Figure 7. - Effect of changing axial gap  $x$  on diffuser effectiveness for a fixed radial gap  $y$  of 0.05 H. Exit rake position,  $L/H$ , 6; diffuser inlet height,  $H$ , 2.54 centimeters; inlet Mach number,  $M_1$ , 0.18.



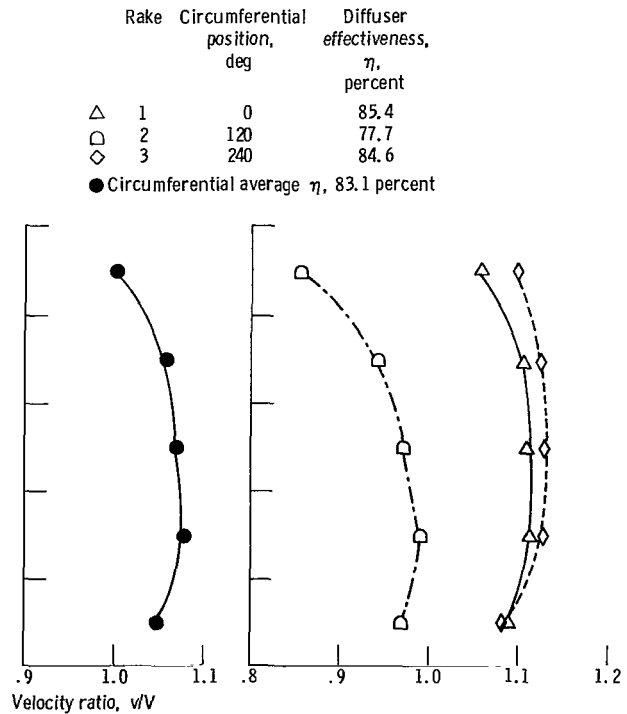
(a) Total suction rate,  $S_t$ , 0; inlet Mach number,  $M_1$ , 0.18.



(b) Total suction rate,  $S_t$ , 0; inlet Mach number,  $M_1$ , 0.41.



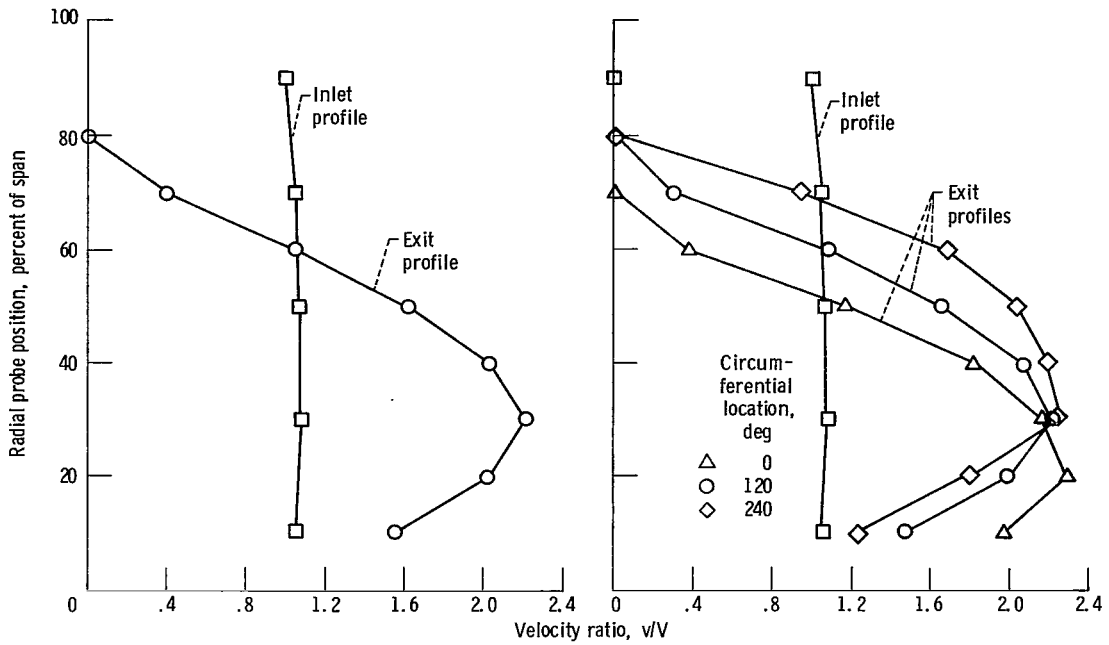
(c) Suction rate at inner wall,  $S_i$ , 5.61 percent; suction rate at outer wall,  $S_o$ , 8.88 percent; total suction rate,  $S_t$ , 14.49 percent; inlet Mach number,  $M_1$ , 0.18.



(d) Suction rate at inner wall,  $S_i$ , 5.65 percent; suction rate at outer wall,  $S_o$ , 8.86 percent; total suction rate,  $S_t$ , 14.51 percent; inlet Mach number, 0.182.

Figure 8. - Variation in radial profiles of inlet velocity at three circumferential locations. Axial gap,  $x$ , 0.3 H; radial gap,  $y$ , 0.05 H; exit rake position,  $L/H$ , 6.

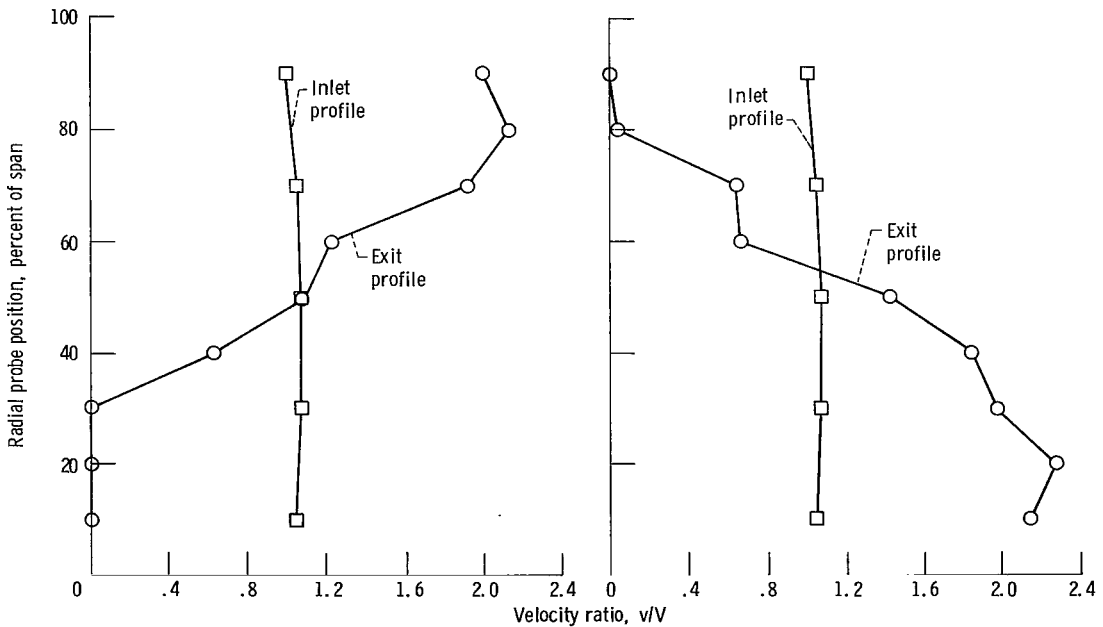




(a) Circumferentially averaged radial profile showing hub weighting.

(b) Radial profiles at three circumferential locations.

Figure 9. - Radial profiles of exit velocity at a total suction rate  $S_t$  of 0. Axial gap,  $x$ , 0.3 H; radial gap,  $y$ , 0.05 H; exit rake position,  $l/H$ , 6; inlet Mach number,  $M_1$ , 0.182.



(a) With tip weighting.

(b) With hub weighting caused by removing suction to outer wall and then restoring suction before recording data.

Figure 10. - Circumferentially averaged radial profile at a total suction rate  $S_t$  of 6.2 percent. Axial gap,  $x$ , 0.3 H; radial gap,  $y$ , -0.02 H; exit rake position,  $l/H$ , 6; inlet Mach number,  $M_1$ , 0.18.

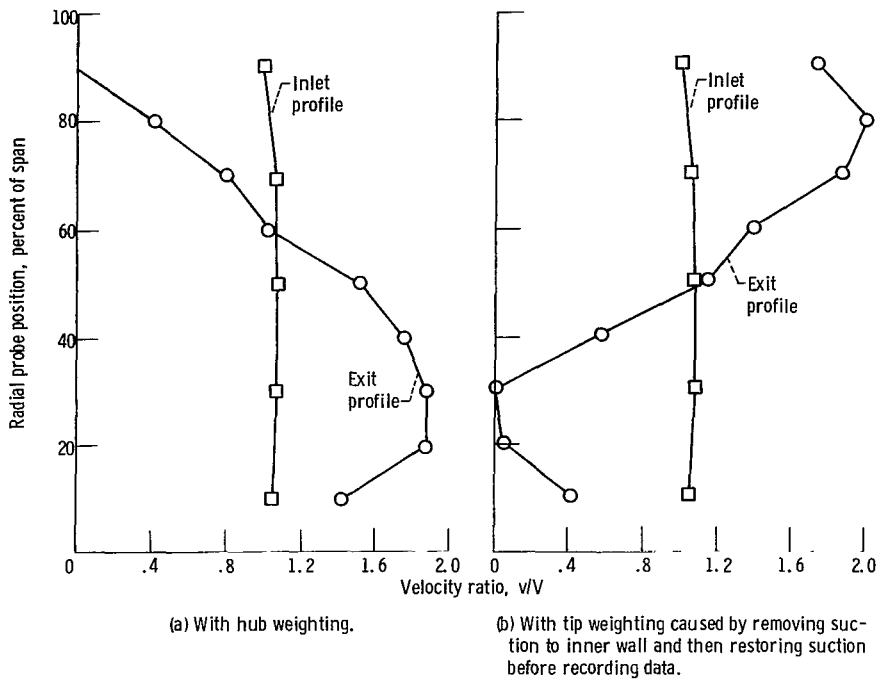


Figure 11. - Circumferentially averaged radial profile at total suction rate  $S_t$  of 5.5 percent. Axial gap,  $x$ , 0.3 H; radial gap,  $y$ , 0.05 H; exit rake position,  $L/H$ , 6; inlet Mach number,  $M_1$ , 0.35.

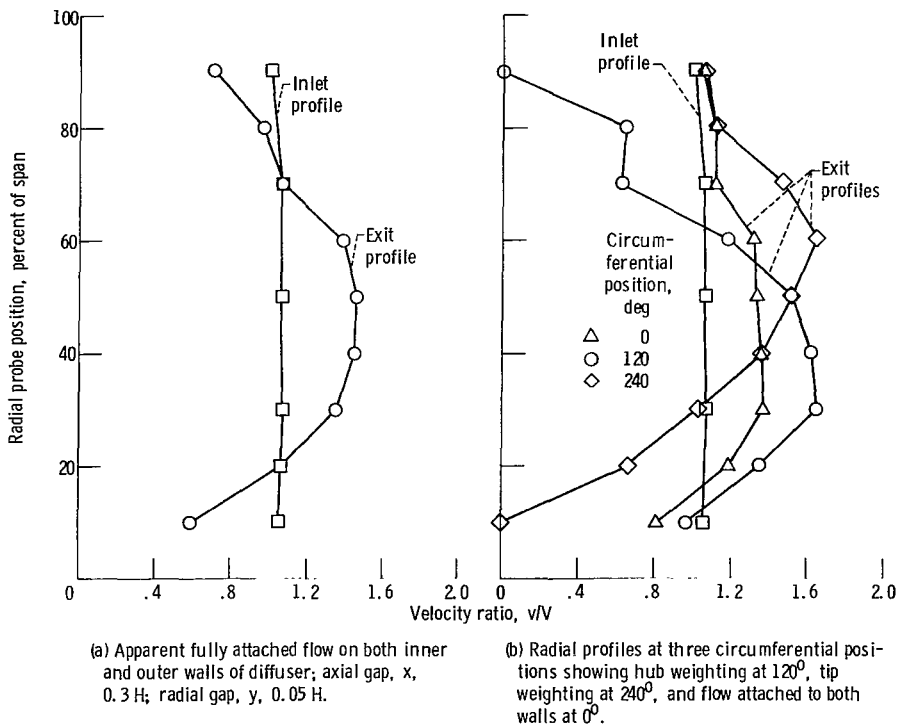
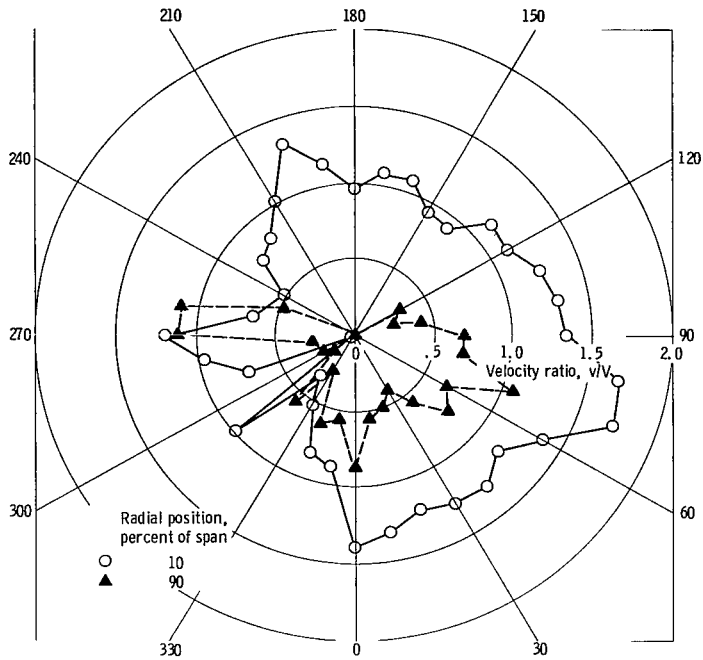
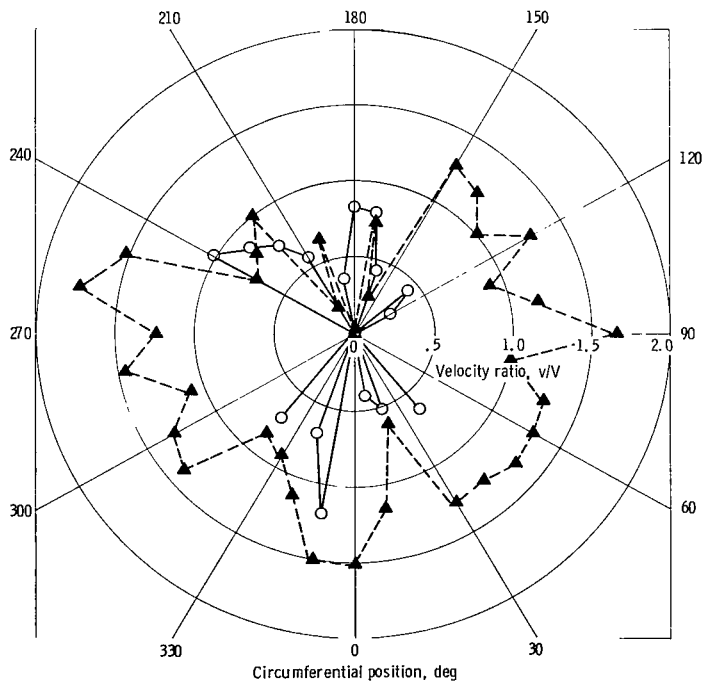


Figure 12. - Circumferentially averaged radial profile at a total suction rate  $S_t$  of 13.7 percent. Exit rake position,  $L/H$ , 6; inlet Mach number,  $M_1$ , 0.183.

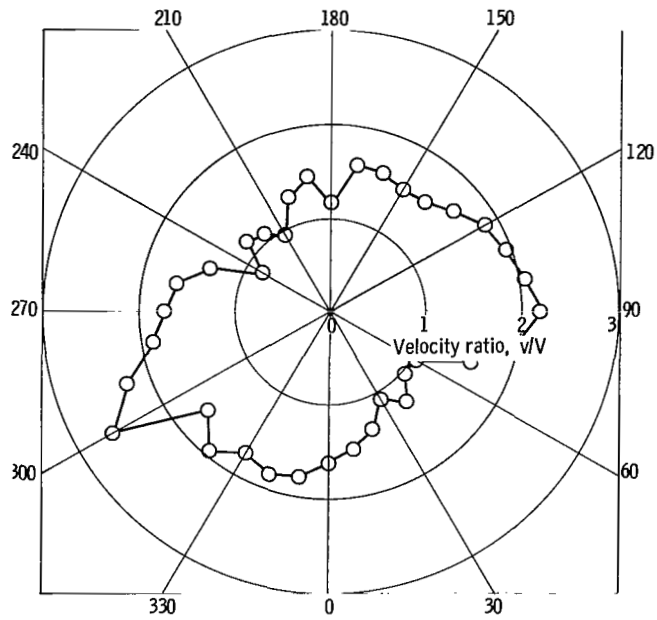


(a) Total suction rate,  $S_t$ , 10.2 percent.

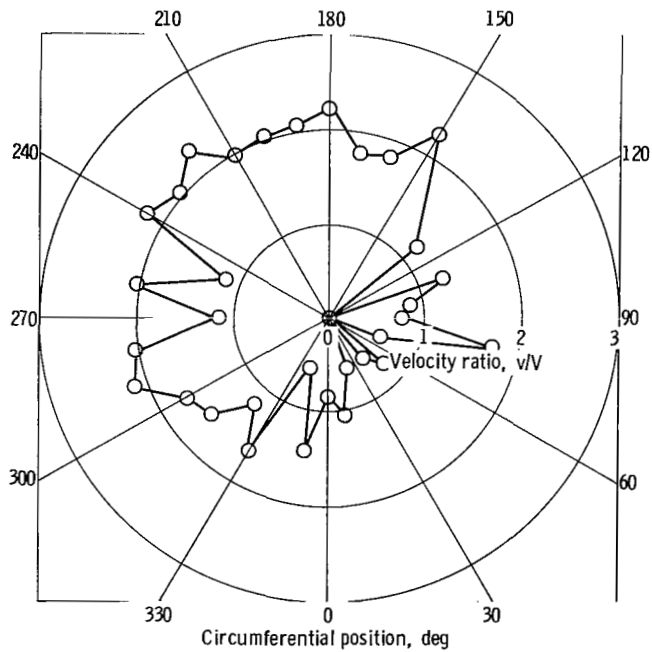


(b) Total suction rate,  $S_t$ , 14.5 percent.

Figure 13. - Effect of circumferential position on local to average velocity ratio at probe positions of 10 and 90 percent of span. Axial gap,  $x$ , 0.3  $H$ ; radial gap,  $y$ , 0.05  $H$ ; exit rake position,  $L/H$ ,  $\xi$ ; inlet Mach number,  $M_1$ , 0.18.



(a) Total suction rate,  $S_t$ , 10.2 percent.



(b) Total suction rate,  $S_t$ , 14.2 percent.

Figure 14. - Effect of circumferential position on local to average velocity ratio at probe position of 50 percent of span. Axial gap,  $x$ , 0.3  $H$ ; radial gap,  $y$ , 0.05  $H$ ; exit probe position,  $L/H$ , 6; inlet Mach number,  $M_1$ , 0.18.

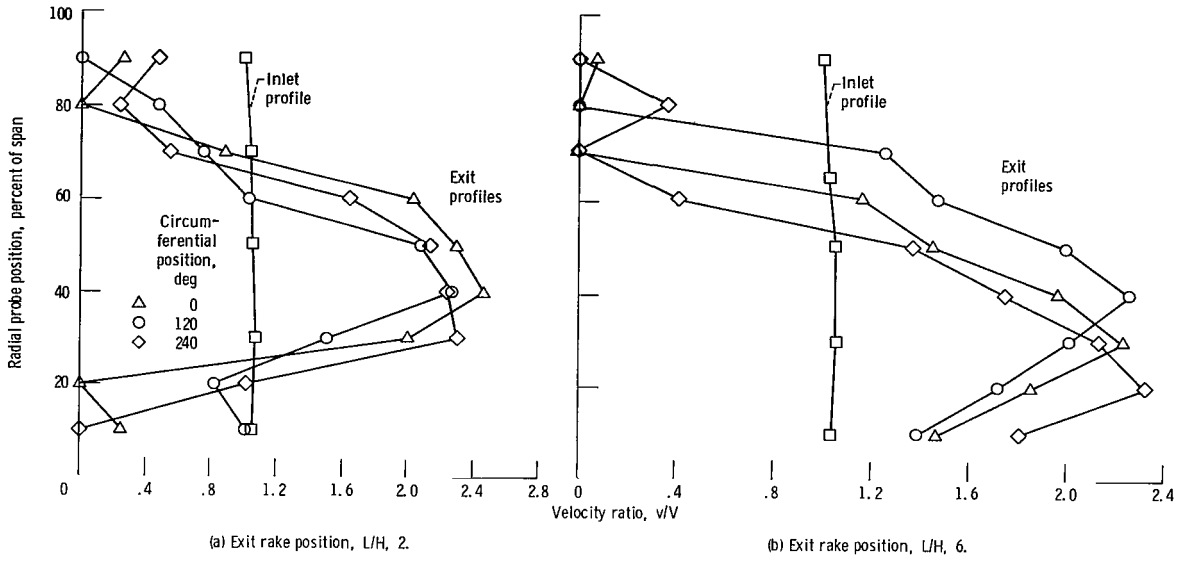


Figure 15. - Radial profiles of exit velocity at two different downstream positions for a total suction rate  $S_t$  of 0. Axial gap,  $x$ , 0.3 H; radial gap,  $y$ , 0.05 H; inlet Mach number,  $M_1$ , 0.183.

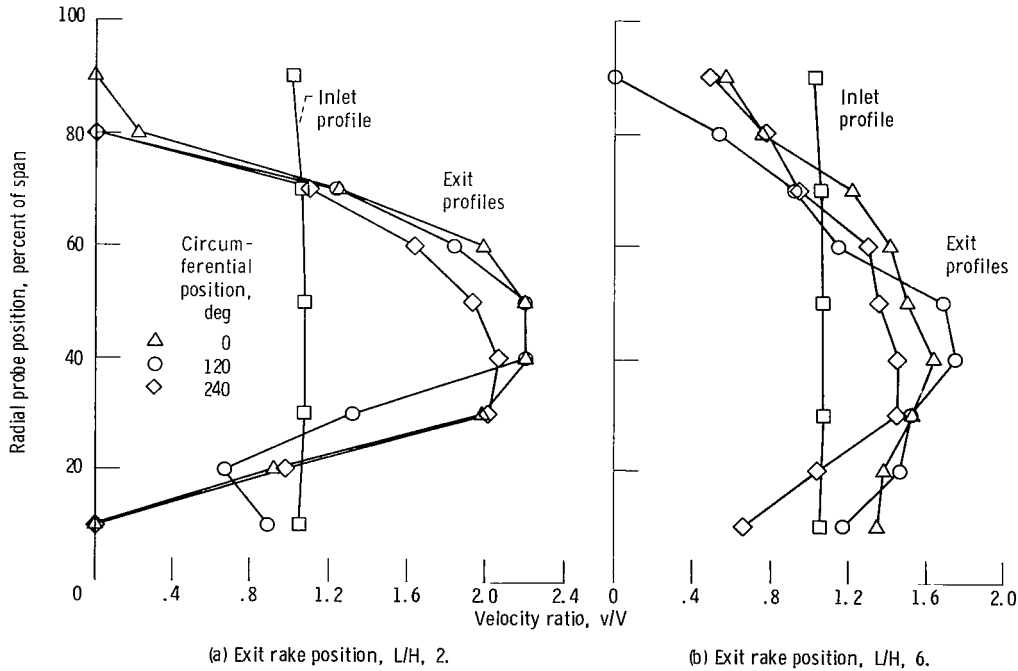


Figure 16. - Radial profiles of exit velocity for nominal suction of 4 percent on inner wall and 6 percent on outer wall. Axial gap,  $x$ , 0.3 H; radial gap,  $y$ , 0.05 H; inlet Mach number,  $M_1$ , 0.183.

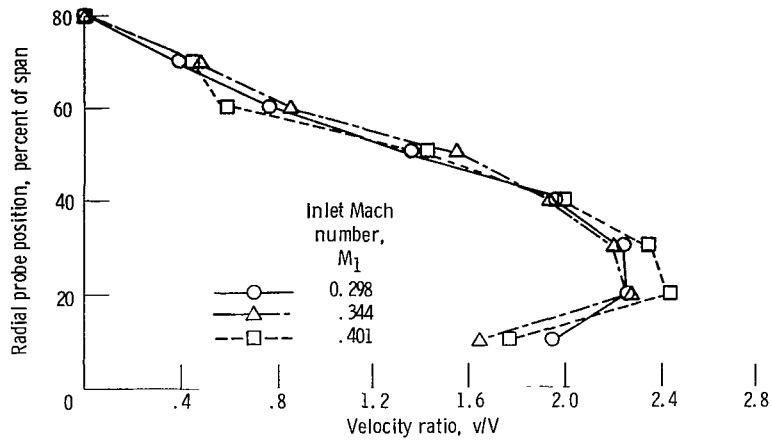


Figure 17. - Radial profiles of exit velocity for three inlet Mach numbers at total suction rate  $S_t$  of 0. Axial gap,  $x$ , 0.3 H; radial gap,  $y$ , 0.05 H; exit rake position,  $L/H$ , 6.

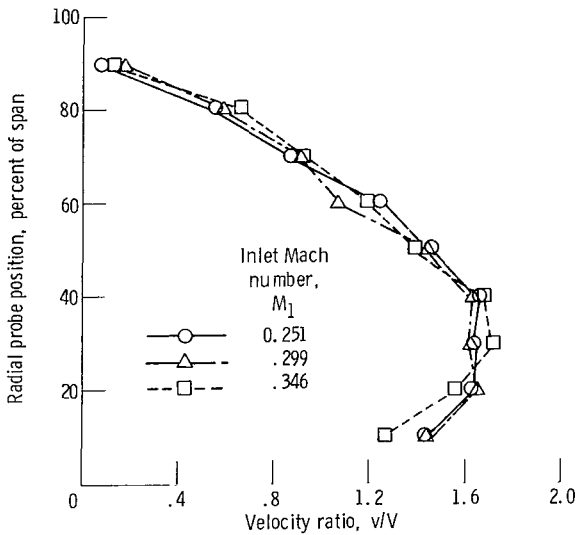


Figure 18. - Radial profiles of exit velocity for three inlet Mach numbers at nominal suction rates of 3 percent on inner wall and 4.5 percent on outer wall. Axial gap,  $x$ , 0.3 H; radial gap,  $y$ , 0.05 H; exit rake position,  $L/H$ , 6.

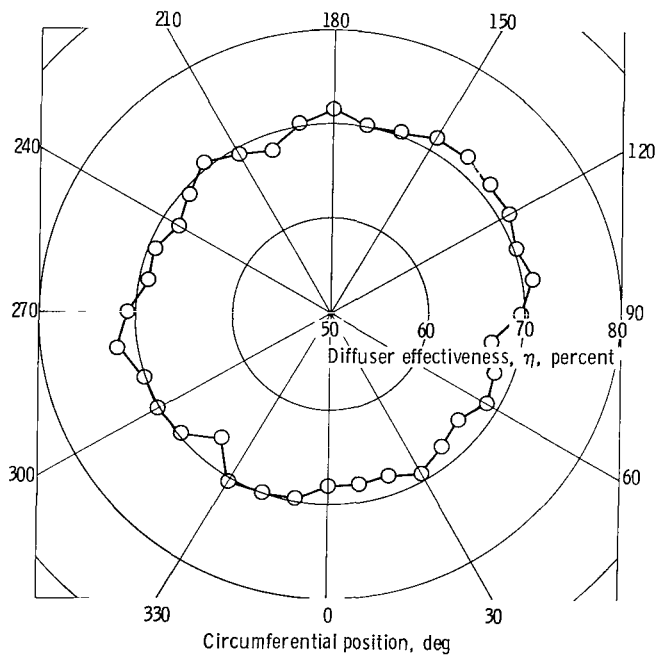


Figure 19. - Effect of circumferential position on diffuser effectiveness for total suction rate  $S_t$  of 10.2 percent. Axial gap,  $x$ , 0.3 H; radial gap,  $y$ , 0.05 H; exit rake position,  $L/H$ , 6; inlet Mach number,  $M_1$ , 0.18.

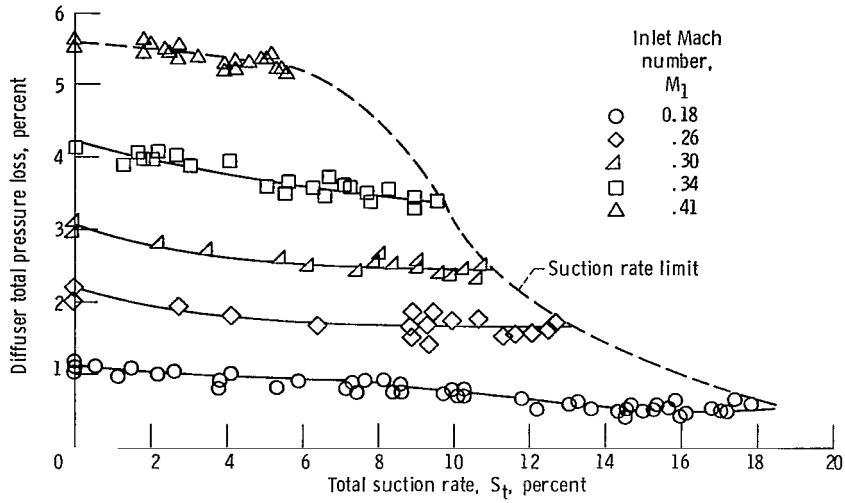


Figure 20. - Effect of total suction rate on diffuser total pressure loss for several inlet Mach numbers. Axial gap,  $0.3 H$ ; radial gap,  $y$ ,  $0.05 H$ ; exit rake position,  $L/H$ , 6.

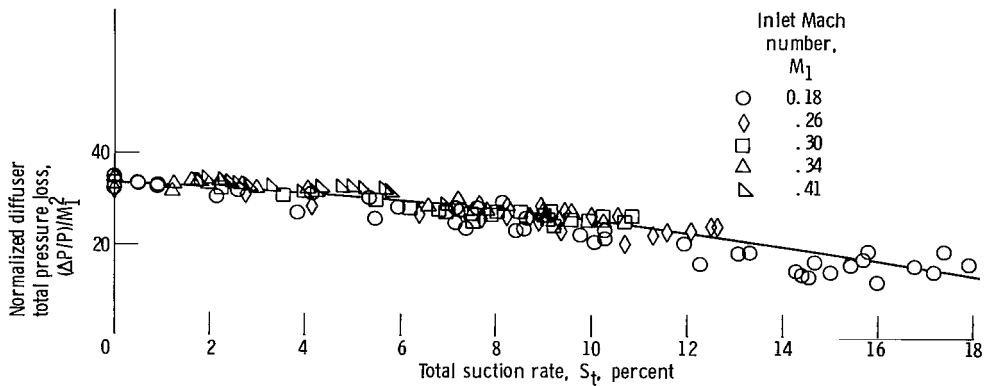


Figure 21. - Effect of total suction rate on diffuser total pressure loss normalized by the square of the inlet Mach number. Axial gap,  $x$ ,  $0.3 H$ ; radial gap,  $y$ ,  $0.05 H$ ; exit rake position,  $L/H$ , 6.

1. Report No. NASA TP-1194	2. Government Accession No.	3. Recipient's Catalog No.
4. Title and Subtitle <b>PERFORMANCE OF A SHORT ANNULAR DUMP DIFFUSER USING SUCTION-STABILIZED VORTICES AT INLET MACH NUMBERS TO 0.41</b>	5. Report Date April 1978	6. Performing Organization Code
7. Author(s) John M. Smith and Albert J. Juhasz	8. Performing Organization Report No. E-9332	10. Work Unit No. 505-04
9. Performing Organization Name and Address Lewis Research Center National Aeronautics and Space Administration Cleveland, Ohio 44135	11. Contract or Grant No.	13. Type of Report and Period Covered Technical Paper
12. Sponsoring Agency Name and Address National Aeronautics and Space Administration Washington, D. C. 20546	14. Sponsoring Agency Code	
15. Supplementary Notes		
16. Abstract A short, annular dump diffuser was designed to use suction to establish stabilized vortices on both walls for improved flow expansion in the region of an abrupt area change. The diffuser was tested at near ambient inlet pressure and temperature. The overall diffuser area ratio was 4.0. The inlet height was 2.54 cm and the exit pitot-static rakes were located at a distance from the vortex fence equal to two or six times the inlet height. Performance data were taken at near ambient temperature and pressure for nominal inlet Mach numbers of 0.18 to 0.41 with suction rates of 0 to 18 percent of the total inlet airflow. The exit velocity profile could be shifted toward either wall by adjusting the inner- or outer-wall suction rate. Symmetrical exit velocity profiles were unstable, with a tendency to shift back to a hub- or tip-weighted profile. Diffuser effectiveness was increased from about 47 percent without suction to over 85 percent at a total suction rate of about 14 percent. The diffuser total pressure losses at inlet Mach numbers of 0.18 and 0.41 decreased from 1.1 and 5.6 percent without suction to 0.48 and 5.2 percent at total suction rates of 14.4 and 5.6 percent, respectively.		
17. Key Words (Suggested by Author(s)) Combustor flow control Vortex diffuser	18. Distribution Statement Unclassified - unlimited STAR Category 07	
19. Security Classif. (of this report) Unclassified	20. Security Classif. (of this page) Unclassified	21. No. of Pages 38
		22. Price* A03